16. Juni 1998

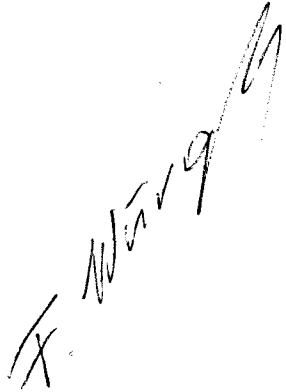# STOCHASTIC AND NON-STOCASTIC EFFECTS OF
BETA-HOT PARTICLES IN TISSUE

A dissertation submitted to the

SWISS FEDERAL INSTITUTE OF TECHNOLOGY ZURICH

for the degree of

Doctor of Natural Sciences

presented by

Martina Noëlle Sigg

Eidg. dipl. pharm.

born 20. 12. 1960

citizen of Dörflingen, SH

accepted on the recommendation of

Prof. Dr. Chr. Schlatter, examiner

Prof. Dr. F. E. Würgler, co-examiner

Prof. Dr. W. Burkart, co-examiner

Dr. N. E. A. Crompton, co-examiner

1997

ACKNOWLEDGEMENTS

CONTENTS:

ZUSAMMENFASSUNG

Sogenannte "heiße Teilchen" sind kleine, hochradioaktive Partikel, zwischen 10 µm und 3 mm groß, unlöslich in Wasser, aber bedingt durch ihre Kleinheit leicht durch die Luft transportierbar. Sie bestehen meistens aus Aktiniden und Spaltprodukten, und ihre spezifische Aktivität kann bis zu Millionen von Becquerel hoch sein. Die erste Publikation über menschliche Strahlenbelastung durch radioaktive Partikel erschien bereits 1958, doch wurde die Thematik vor allem durch die Reaktorkatastrophe von Chernobyl aktualisiert.

Die Deposition eines heißen Teilchens auf menschlichem Gewebe (v.a. Haut, Lungenoberfläche, Gastrointestinaltrakt) wirft sowohl aus dosimetrischer, wie auch aus strahlenbiologischer Sicht einige Probleme auf, die mit den üblichen Modellen nicht gelöst werden können. Wird die applizierte Dosis über ein ganzes Organ oder über den ganzen Körper gemittelt, so wird sie verschwindend klein. Die α- und β-Teilchen, die beim Zerfall der Nuklide entstehen, haben im Gewebe nur eine sehr beschränkte Reichweite. Im Gegensatz zum α-Teilchen, das seine ganze Energie innerhalb weniger µm deponiert, verliert ein β-Teilchen seine Energie konstant, d.h. es kommt zu einem Energiegefälle innerhalb seiner maximalen Reichweite von wenigen mm. Das bedeutet, dass abhängig von der Gesamtaktivität und von der Art des β-Nuklids, Zellen ab einer gewissen Distanz nicht mehr lethal geschädigt werden. Ionisierende Strahlung kann verschiedene Effekte auf zellulärer Ebene haben, sie entstehen entweder direkt durch Interaktion mit der DNS oder nach der Bildung freier Radikale, die wiederum die DNS oder andere zelluläre Strukturen schädigen können. Beinahe jede Zelle hat die Fähigkeit, entstandene Schäden bis zu einem gewissen Grade zu reparieren. Ist die Reparatur unvollständig, aber die Zelle bleibt reproduktionsfähig, so resultieren mutierte oder transformierte Zellen, dies kann je nachdem genetische Mutationen oder Krebs ergeben.

Bei Tierversuchen mit heißen Teilchen auf der Haut konnte in vielen Fällen außer einer Nekrose nichts beobachtet werden, doch gab es auch einige Hinweise darauf, dass Mutationen in überlebenden Zellen stattgefunden haben. Die Entstehung eines Tumors ist ein mehrstufiger Prozeß, bei dem im Tiermodell nur das Endprodukt bewertet werden kann, die Vorstufen aber nur sehr bedingt erkannt werden können. Hier bietet das Zellkulturmodell einige Vorteile, da es sich viel besser eignet, um mechanistische Studien zu betreiben. Insbesondere die C3H 10T1/2 Maus Fibroblasten bieten sich an als weltweit anerkanntes und reproduzierbares System zur Untersuchung von

Transformationen. Diese Zellen wachsen unter normalen Bedingungen nur so weit, bis sie andere Zellen berühren. Man spricht von einer Kontaktinhibition. Die Zellen können durch verschiedenen Agentien transformiert werden. Dadurch verlieren sie ihre Fähigkeit zur Kontaktinhibition, sie bilden sogenannte Foci, das sind Zellwucherungen, die sich klar vom nicht transformierten Zellrasen abheben. Das Hauptziel dieser Dissertationsarbeit war es also, ein Zellkulturmodell zu entwickeln, in dem Effekte heißer Teilchen untersucht werden können. Aus theoretischen Überlegungen war es sinnvoll, als Strahlenquelle einen β-Emitter zu wählen, und zwar in einer solchen Aktivität, dass gewisse Zellen tödliche Dosen erhalten, die meisten Zellen aber nicht tödlich geschädigt werden. Die Frage war dann, ob die Schädigung der letzteren stärker oder schwächer ist verglichen mit einem System, in dem alle Zellen die selbe Strahlendosis erhalten.

Als Strahlenquelle wurde ein schmaler Yttriumdraht gewählt, der durch Neutronenbeschuss aktiviert wurde. Das entstandene Y-90 ist ein reiner β-Emitter. Der Draht wurde unterhalb einer Zellkulturplatte mit einem speziell dünnen Boden fixiert. Die errechnete wie auch die gemessene Dosimetrie ergaben ein extrem inhomogenes Strahlenfeld, mit 24 h-Dosen direkt über dem Draht von mehr als 750 Gy, die mit Distanz sehr schnell abnahmen bis zu 0 Gy bei ca. 20 mm Abstand. Als biologische Versuche wurden Überlebenstests und Transformationsstudien unternommen. Für die Überlebenstests wurden die Zellen in Abständen von jeweils 1 mm isoliert und ihre Reproduktionsfähigkeit bestimmt. Die so gemessenen Überlebensraten ergaben eine klare Übereinstimmung mit dem extremen Dosisabfall.

Mit Hilfe dieser Tests konnte die Zone bestimmt werden, in der die Überlebensrate so zwischen 60 und 70 % war, ein Bereich, in dem Transformationen wahrscheinlich sind. Im inhomogenen Yttriumsystem war dies in 9 bis 11 mm Abstand vom Draht. Die Zellen in diesem Bereich wurden nach der Bestrahlung isoliert und ihre Transformationsrate wurde bestimmt. Die Transformationsrate betrug 1 transformierte Zellen pro 1'000 überlebende Zellen. Im Vergleich dazu wurde die Transformationsrate von Zellen bestimmt, die im genau gleichen Dosisbereich wuchsen, die aber während der Bestrahlung isoliert waren. Sie betrug 1 transformierte Zelle auf 10'000 Zellen, war also 10 x niedriger als im anderen System. Dies bedeutet also, dass im ersten System, in dem während der Bestrahlung Zellen mit unterschiedlichen Schädigungen Kontakt untereinander haben, die Transformationsrate höher ist, als wenn dieser Kontakt nicht stattfinden kann.

Diese Dissertationsarbeit umfaßt auch Untersuchungen von transformierten C3H 10T1/2 Zellen. Die Zellen wurden isoliert und kloniert. Darauf wurde ihre DNS-Verteilung, ihre Strahlenempfindlichkeit und ihre genomische Instabilität untersucht. Die verschiedenen Klone zeigten sehr unterschiedliche DNS-Verteilungen. Einige waren extrem unstabil. Die Strahlenempfindlichkeit von transformierten Zellen war gegenüber nicht transformierten Zellen nicht verändert.

SUMMARY

So called hot particles are small and highly radioactive fragments, with a diameter between 10 μm and 3 mm, insoluble in water and small enough to become airborn. Generally, they are made up of fission products or actinides with a specific activity of up to millions of Becquerels. The first article about human exposure due to radioactive particles was published in 1958, but the main discussion about human risk due to hot particles started after the Chernobyl catastrophy in 1986.

The desposition of a hot particle onto human tissue (mainly skin, lung surface and gastrointestinal tract) poses problems, which cannot be solved with current models of dosimetry and radiobiology. Alpha- and β-particles have only a defined range in tissue. Contrary to α-particles, which deposit their energy within a few microns, β-particles gradually loose their energy within a few millimeters. Therefore, the dose distribution around β-hot-particles is skewed, so that cells in the nearest vicinity receive an extremely high dose, but cells a few cell-diameters distant receive much lower doses. In such a situation, averaging dose over the whole organ or whole body underestimates the exposure situation.

Ionizing radiation damages living cells. It has been postulated to induce its multiple biological effects either by direct interaction with DNA or through the formation of free radical species and subsequent interaction with DNA or other cellular structures. Cells have the capability to repair DNA-damage. Incomplete repair can result in mutated or transformed cells, and later in mutations or cancer.

Experimental exposure of animal skin to hot particles induces primarily tissue necrosis, but there are some indications of mutations induced in surviving cells. Evolution of a tumour is a multistep process and in animal experiments only the final product, the tumour, can be evaluated. In cell culture models, however, the mechanisms involved in the transformation process can be examined. Particularly the C3H 10T1/2 mouse fibroblast transformation assay is recognized worldwide as a reproducible and acceptable cell model. Under normal growth conditions, the C3H 10T1/2 cells stop dividing after touching neighbouring cells, a process referred to as contact inhibition. The cells can be transformed by diverse agents, and after transformation they loose contact inhibition and build so called foci, which are cell aggregates clearly distinguishable from the untransformed monolayer of parent cells. The main aim of this thesis was to develop a cell culture model which permits

investigations of hot particle effects. On theoretical grounds a β-emitting radiation source was chosen. The activity should be sufficiently high, so that some cells receive a lethal dose, but most cells should not be lethally damaged. The question to be answered was whether in such a system the damage was higher than in a system where all cells receive the same radiation dose.

As a radiation source, a small yttrium-wire was chosen, which was activated by thermal neutrons. Y-90 is a pure β-emitter. The wire was fixed below a cell culture plate with a thin basement growth foil. The estimated and measured dosimetry yielded an extremely inhomogeneous radiation field, with 24-hour doses directly above the wire of more than 750 Gy, rapidly decreasing to 0 Gy within 20 mm. As biological endpoints, survival and transformation rate were determined. For the survival assay, cells at 1 mm distances were isolated and their reproducibility was determined. The measured surviving fraction reflected the extreme decrease of dose.

The area displaying a surviving fraction between 60% and 70% (between 9 and 11 mm distance from the wire) was chosen for investigation with the transformation assay. After irradiation, the cells in this area were isolated and their transformation rate was determined. One transformed cell per 1'000 surviving cells was observed. For a control, the transformation rate was determined of cells growing in the same dose area but being isolated during the irradiation. Here, the transformation rate was 1 transformed cell per 10'000 surviving cells, 10 times lower than in the other system. This means that the transformation rate is higher in a system permitting between differently damaged cells contact during irradiation than in a system without such contact.

The thesis also describes investigations of transformed C3H 10T1/2 cells which have been isolated and cloned. The investigations of their DNA distribution, their radiation sensitivity and their genomic instability showed very different DNA distributions in the various clones. Some of the clones were genetically extremely unstable. Radiation sensitivity, however, was identical when compared with untransformed cells.

1. INTRODUCTION

A hot particle is defined as "a discrete radioactive fragment with a high specific activity (at least 3700 up to millions of Becquerels), insoluble in water, and not larger than approximately 3 mm in any dimension but greater than 10 μm" [1], [2]. Generally, it is made up of insoluble fission products or actinides, and small enough to become airborne. Hot particles are present *e.g.* in reactor facilities and in nuclear fallouts.

On the 26th of April 1986 the fourth reactor block at Chernobyl exploded and then burned for several days. This brought enormous amounts of radioactive material into the atmosphere [3]. A large fraction of the local fallout consisted of small, insoluble and highly radioactive particles that were transported through the atmosphere and deposited all over Europe. The hot particles of the Chernobyl fallout consisted mostly of ruthenium-103 and -106, chromium-51, molybdenum-99, technetium-99m, curium-242, niobium-95 with activities of up to 10 kBq [4, 5]. These nuclides are mainly β-emitters. Human exposure of such particulate radioactivity occurs via ingestion, inhalation or deposition on the skin. The hot particle acts like a little radiation source with a high specific acticity. A β-particle has a range of up to a few millimetres in tissue, gradually loosing its energy. Therefore, the dose distribution is skewed, so that cells in the nearest vicinity receive an extremely high dose, but cells a few cell-diameters distant receive much lower doses. In such a situation, averaging dose over the whole organ or whole body does not properly reflect the exposure situation.

Ionizing radiation damages living cells. It has been postulated to induce its multiple biological effects either by direct interaction with DNA or through the formation of free radical species and subsequent interaction with DNA or other cellular structures. Some of these initial changes may have both short- and long-term consequences, depending on the ability of the cells to repair their DNA. If cellular damage occurs and is not adequately repaired, it may prevent the cell from surviving or reproducing, or it may result in a viable, but modified cell, *i.e.* mutated or transformed. Late effects of radiation exposure result from cells that survive but retained some legacy [6]. If the harmed cell is a germ cell, the change may be a genetic mutation, if it is a somatic cell, the result may be cancer. Epigenetic effects include interactions between cells, *e.g.* loss of intercellular signalling [7]. These may be passed onto the progeny, and can increase or reduce subsequent effects at the tissue or organ level.

Biological effects of radiation are also categorized into stochastic and non-stochastic effects. A stochastic effect is governed by the laws of probability. It arises from the injury of a few cells, or even a single cell. Increasing radiation dose does not increase the severity of a stochastic effect but does increase the probability of the effect in a population. A stochastic effect is an all-or-none effect and has no dose threshold. Mutation or cancer are examples of a stochastic effect. Nonstochastic or determenistic effects increase in severity with increasing dose, a threshold exists. Typical nonstochastic effects include cataracts, fibrosis or loss of proliferative capability, also in stem cell populations [6].

Hot particles produce various stochastic and non-stochastic effects in tissue. Only a few cells per particle receive an extremely high dose at a high dose-rate which leads to acute cell death or loss of proliferative capacity. A microlesion arises at these sites. In the case of α-particles, the dose outside this area is practically zero. Most of the dose is deposited to already damaged cells, so that an "overkill" situation arises. Due to the longer penetration depth of β-particles the picture becomes more complex: Within biochemical signalling range of the superlethally irradiated area are cells which receive sublethal radiation doses as well as growth stimuli due to tissue response to the microlesion.

Defined limits for partial organ irradiation by hot particles exist for the skin [2], however uptake via ingestion or inhalation is also possible, leading to irradiation exposure of lung and gastrointestinal tract. NCRP on „Limits for exposure to hot particles" (draft [1]) considers for the skin, eye, ear and anterior nose deterministic effects to be most important, first of all ulceration. The recommended dose limit is 0.5 Gy at a depth of 70 μm (7 mg cm^{-2}) averaged over the most highly exposed 10 cm^2. For the gastrointestinal and the respiratory tract, also stochastic effects are possible and important to control. However, there is currently no dosimetry model designed specifically for evaluating the absorbed dose distribution to the respiratory tract arising from a single hot particle.

The respiratory system is a complex arrangement of organs and tissues whose primary function is the intake of oxygen and the eliminiation of carbon dioxide. The respiratory tract can be separated into two parts, based on gross anatomy and physiology: (1) the proximal-conducting, nonrespiratory airways that include the nose, pharynx, larynx, trachea, bronchi, and nonalveolarized bronchioles; and (2) the distal respiratory region (*i.e.* respiratory bronchioles, alveolar ducts, and alveoli). Gas exchange between blood and air is restricted to the resrpiratory region [1]. Except of the alveolar ducts and alveoli, all airways are

lined with mucus-covered ciliated cells. The mucus decreases in thickness with the increase in the generation number. Mucociliary clearance allows the transfer of deposited particulate matter into the gastrointestinal tract [8]. The deposition of an inhaled particle is dependent on various factors, *e.g.* breathing rate and characteristics, composition of mucus, ciliary movement, and particle characteristics (size, shape, weight and solubility) [9]. Clearance occurs either via mucociliary movements towards the pharynx and following ingestion, or via macrophage digestion. The deeper the deposition in the bronchial tree, the slower the clearance mechanism [10]. In smoker lungs or pathological parenchyma's the clearance mechanism is disturbed because most ciliar cells are dead are destroyed. The retention of a hot particle on the lung surface and therefore the irradiation time can last between a few hours and up to several days or months, leading to very high doses to only a few cells.

The critical target cells in the lung epithelium sensitive to transformation into tumor cells are those able to proliferate. Therefore, proliferating basal cells and non-ciliated columnar cells are considered to be at risk for stochastic effects [8]. The assessment of risk for β-hot-particles is difficult because both non-stochastic and stochastic damage occurs, and because of the tissue dynamics of the afflicted lung epithelium. Close to the hot particle the dose is so high that mainly non-stochastic damage occurs. But outside this area, within a few cell diameters, dose and dose-rate are much lower and stochastic effects predominate. This special situation makes the use of standard dose-effect models inappropriate. In the UNSCEAR report (1993) [11] "on the influence of dose and dose rate on stochastic effects of radiation", three basic non-threshold dose effect models are discussed: the linear, the linear quadratic, and the pure quadratic model. The best fit of most data on radiation effects of cells and tissues including cell killing, the induction of chromosome aberrations, mutation, cell transformation and tumor induction, was considered to be to a linear-quadratic equation, although in a number of experimental studies linear functions also gave reasonable fits. ICRP [12] and NCRP [13] exposure limitation systems considered the risk of stochastic effects to be a linear, non-threshold function of equivalent dose.

These models were based on experimental and epidemiological data, but did not consider the special situation of hot-particle irradiation. In the hot-particle situation many factors can promote the multistep process of carcinogenesis, and enhance the probability for tumor-progression. This can cause the dose-effect curve to change from linear to quadratic or even higher terms. Uncertainties about risks from α- and β-particles have been discussed since

1960. These contributions are reviewed briefly on p. 30, by Lang *et al.* [*14*], and in the NCRP draft [1].

The limited experimental data available of *in vitro* β-irradiations give rise to the hypothesis that conventional dose risk assessment models underestimate the biological significance of β-emitting hot particles. Rytömaa *et al.* [15, 16] added isolated β-hot-particles directly to a monolayer of C3H 10T1/2 cells and observed a 100% induction of transformation. All transformed cells were within 2 - 4 mm of the radiation source. They observed death of the surrounding cells, an enhanced mitotic activity of cells around the lethal zone, and an overexpression of p53 in the transformed cells as well as in hot particle-induced tumors in mouse epidermis.

The aim of the present dissertation was to develop a cell culture system to investigate the effects of inhomogeneous radiation fields, *i.e.* radiation fields with distinct dose variations within few cell diameters. The advantages of a cell culture system are high reproducibility and an exact dosimetry. Short lengths of yttrium-89 wires were neutron activated to yttrium-90 for use as β-radiation sources. One active wire was attached below the cell culture dish to produce an extremely inhomogeneous radiation field.

To quantify non-stochastic effects, clonogenicity of the cells as a function of distance from the β-source was determined. In these experiments M3-1 cells were used because they are a particularly amenable line of fibroblasts for survival assays. From these experiments sublethal and the superlethal dose regions could be specified.

As an end-point for stochastic effects cell transformation studies were performed using C3H 10T1/2 fibroblasts. The transformation rate was determined in the sublethal dose region of the inhomogeneous radiation field and compared to cells that received the same dose and dose rate but in the absence of heavily damaged cells.

The C3H 10T1/2 transformation assay is well established. C3H 10T1/2 Clone 8 is a nontumorigenic fibroblast cell line derived from the embryonic tissue of an inbred C3H mouse. It was established in culture by Reznikoff [17, 18]. Although these cells are immortalized, they exhibit contact-inhibition control over cell division. The chromosome complement is hypotetraploid. Upon transformation they loose contact inhibition and form dense, discrete foci of actively growing transformed cells which can be recognized morphologically and which produce tumors when transplanted into nude mice. The many positive attributes of this cell line as well as the relative ease in performing the transformation assay have made it one of the primary systems for examining mechanisms involved in

the transformation process. Some suspects of transformation that have been investigated with C3H 10T1/2 cells include initiation and promotion [19, 20, 21], the role of the cell cycle in carcinogen sensitivity [22, 23, 24], inhibition of transformation [25], and the role of intercellular communication in the transformation process [26, 27]. Many authors have used 10T1/2 cells to determine dose- and dose-rate-effect relationships for chemicals [28], ionizing and non-ionizing radiation [29, 30, 31]. The assay must, nevertheless, be conducted in a very precise manner, since many parameters can influence transformation rate [32].

Kennedy *et al.* [33] demonstrated that following a 4 Gy dose of X-rays, transformation frequency was independent of the number of cells irradiated. They concluded that some change was induced by the radiation exposure which was transmitted to the progeny of the surviving cells and resulted in an enhanced frequency of morphological transformation. In order to check genomic-instability, radiation-induced neoplastic transformants were isolated and cloned. DNA content and cell cycle blocks after X-rays were investigated.

2. MATERIALS AND METHODS

2.1 *Cell culture*

M3-1 Chinese hamster bone-marrow cells (originally supplied by Dr. M.R. Raju, Los Alamos, USA), were grown in MEM-α (Gibco), supplemented with 10% fetal bovine serum (Seromed), penicillin (25 units ml^{-1}) and streptomycin (25 µg ml^{-1}). Cultures were kept in a humidified atmosphere of 95% air, 5% CO_2 at 37°C.

C3H 10T1/2 clone 8 mouse embryo fibroblasts were obtained from Dr. L. Hieber, GSF Zentrum für Umwelt und Gesundheit, Munich, Germany, at passage 8. The cells were grown to passage 9 and then frozen in liquid nitrogen.

The stock cultures were grown in 75 cm^2 flasks and were never allowed to reach confluence. Only cells below passage 15 were used. The cells were maintained in BME medium (Amimed, Switzerland), 10% heat-inactivated fetal bovine serum (various sources, see below) and 0.5% gentamycin (Amimed), at 6% CO_2 and 37°C. The serum can have a significant influence on growth characteristics. Therefore, great care was given in selecting a serum lot. Different lots from various sources (Boehringer, Seromed, Amimed) were screened by measuring growth rate and clonogenicity after 4 Gy X-ray (see later for exact details of survival assay). All yttrium transformation assays were performed using the same lot (Boehringer Mannheim, Germany). The serum was heat inactivated at 56°C for 30 minutes before adding to the medium.

2.2. *Standard assay, C3H 10T1/2:*

2.2.1. Irradiation X-ray, high dose rate

C3H 10T1/2 cells were irradiated 24 hours after plating in flasks. The cells were in exponential growth. Irradiation was performed with 240 kV X-rays and 6.3 mA current (Philips MCN 321 X-ray tube, Philips, Hamburg). Doses were determined with a Farmer ionization chamber (NE 2571, Nuclear Enterprises, Reading, England). The dose-rate was 0.9 Gy min^{-1}.
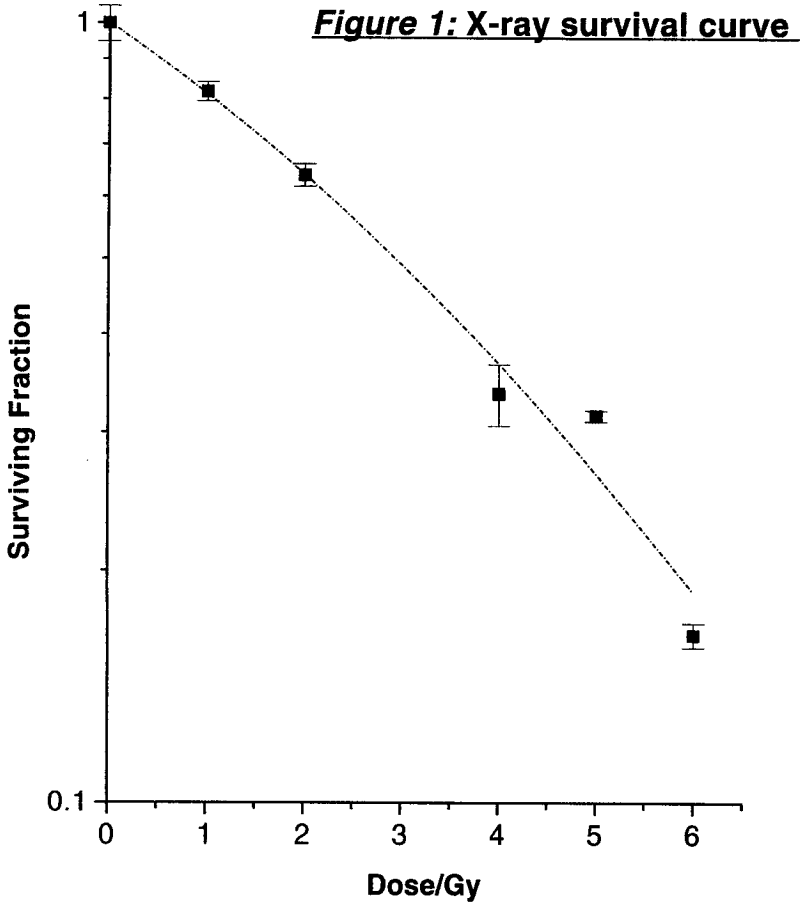
Figure 1: Surviving fraction *versus* total dose (X-ray, 0.9 Gy min^{-1}) for C3H 10 T1/2 cells. Each point represents the mean ± standard errors of 10 to 12 independent experiments. The dashed line is the best fit to the data and is a linear-quadratic curve with α = 0.19 ± 0.03 Gy[-1] and β = 0.02 ± 0.007 Gy[-2] .

2.2.2. Survival

Immediately after irradiation cells were trypsinized, counted and diluted into 9 cm dishes at a concentration of about 50 surviving cells per dish. The dishes were incubated for 9 days and then fixed with methanol and stained with Giemsa (10%, Merck, Switzerland). Colonies with more than 64 cells were counted as survivors. The plating efficiency was 40% ± 5.31. The surviving fraction was determined by dividing the colony numbers of the irradiated dishes by the colony numbers of the control dishes, corrected for initial cell concentrations. The standard survival curve is presented in fig. 1. The best fit to the data is a linear-quadratic curve with $\alpha = 0.19 \pm 0.03$ Gy^{-1} and $\beta = 0.02 \pm 0.007$ Gy^{-2} [34].

2.2.3. Transformation

Immediately after irradiation, cells were trypsinized and diluted into 9 cm dishes. The best cell concentration yields 1.5 - 4 surviving cells per cm^2 [35]. For each experiment between 30 and 100 transformation dishes and 5 survival dishes were prepared to determine the surviving fraction. Transformation dishes were incubated for six weeks with weekly renewal of the medium. Confluency was reached after about 14 days. The medium change was carefully performed in order to avoid contamination or damage of the cell-layer. Cells were washed with PBS, fixed with methanol and stained with Giemsa (10%, Merck). Cellular neoplastic transformation was scored using the morphologic criteria described by Reznikoff [16], which distinguish three different types of foci that clearly stand out against the background (fig. 2): Type I foci are regions of the culture characterized by dense packing of the monolayer (fig. 3). Multilayered areas, 2 to 3 cell-layers deep, are occasionally evident. The periphery of type I foci usually seems rather to blend into the surrounding monolayer of untransformed cells than to grow over the monolayer. The cells within type II foci usually display modest tissue-polarity and do not exhibit a pronounced criss-cross pattern (fig. 4). Extensive cell-piling is usually evident in the densely staining focus interior. Type III foci are characteristically composed of very polar, deeply staining cells actively proliferating over the surrounding monolayer (fig. 5). Criss-cross patterns of growth are evident at the focus periphery while the internal portions of the focus are composed of

multiple cell layers. Only foci of type II and III were counted as transformants. If different parts of the same focus expressed different morphologic characteristics, the focus was assigned to the predominant type. Only foci with a diameter larger than 3 mm were scored. Foci at the edge of the dish were not scored, because they might have been caused by damage to the cell-layer during medium change.

Transformation frequencies were calculated according to the method described by Han and Elkind [36]. They assume that the induced foci are distributed among the transformation dishes with Poisson probabilities. λ is the mean number of foci per dish and is the negative natural logarithmic of the division of the total number of dishes without foci (n) by the total number of dishes (M) ($\lambda = -\ln\frac{n}{M}$). This is a conservative method that might underestimate the transformation frequency, but it avoids inappropriate counting of satellite foci which are often observed and are artefacts produced by cells migrating from the original focus. The transformation frequency is then calculated by dividing λ by the average number of survivor per dish. Standard errors are calculated according to the method of Balcer-Kubicek et al. [37]($SE = \pm\sqrt{\frac{1}{n} - \frac{1}{M}}$)

For each experiment between 10 and 50 control dishes were also prepared. The X-ray, high dose-rate transformation curve is presented in Fig. 6. The best fit to the data is a linear-quadratic curve with α = -0.001 $\pm$ 0.0003 Gy^{-1} and β = 0.00005 $\pm$ 0.00003 Gy^{-2}.
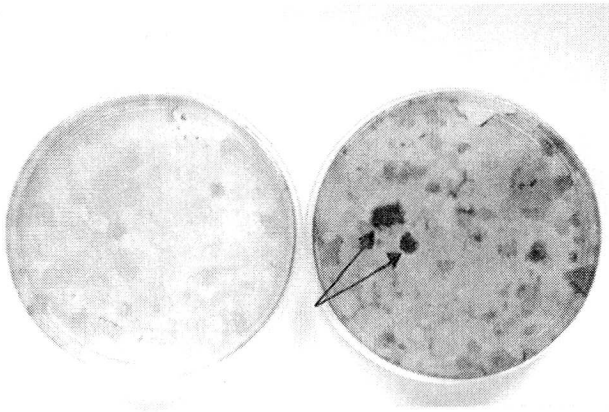
Figure 2: Transformation Dishes

Figure 2: Two confluent C3H 10T1/2 dishes, stained with giemsa, after the 6 week transformation assay (transformed with X-ray, 4 Gy, high dose rate); Left dish with no foci, right dish with two clearly defined foci (marked with arrow).

Figure 3: Focus Type I
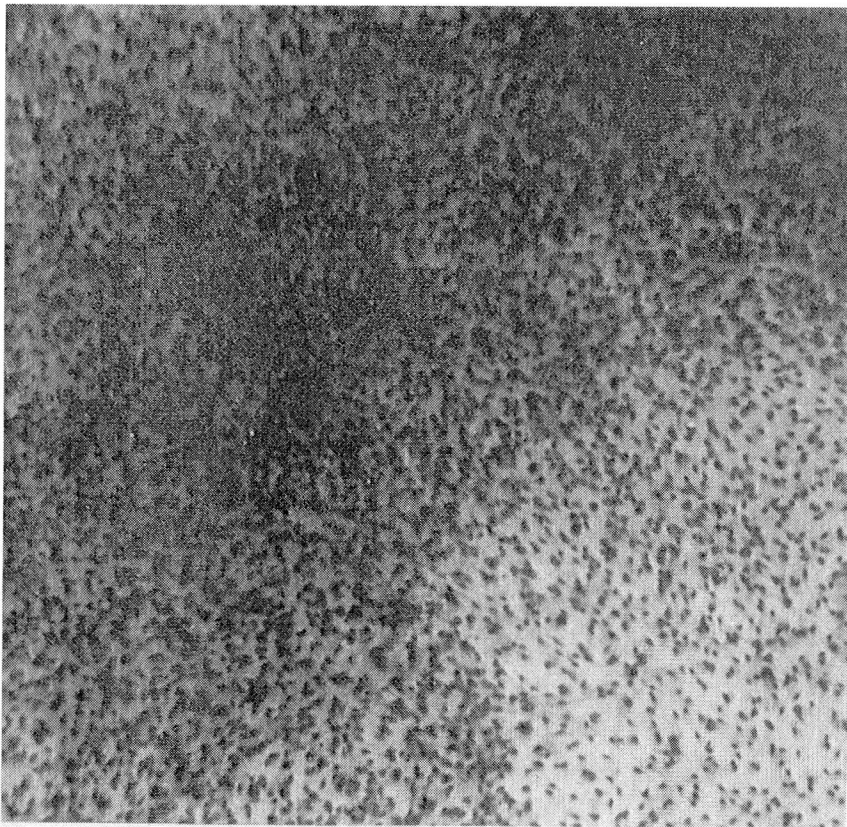
Figure 3: Photomicrograph of the edge of a focus type I (25x). This type is characterized by densely packed C3H 10 T1/2 cells. Cells at the periphery of the focus do not grow over the monolayer.

Figure 4: Focus Type II
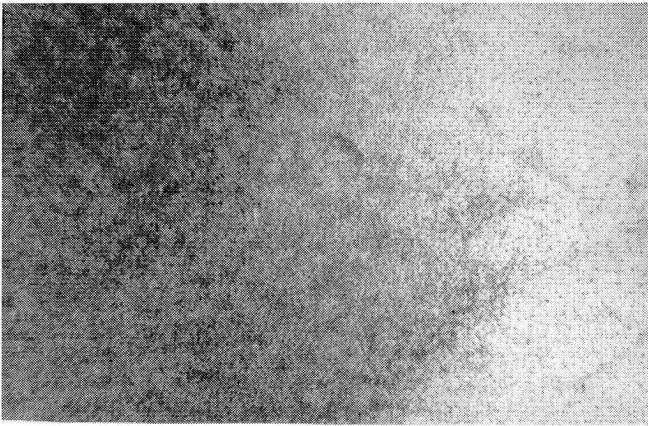
Figure 4: Photomicrograph of the edge of a focus type II (15x). Extensive cell piling is evident in the interior part and transformed cells grow over the monolayer of untransformed cells surrounding the focus.

Figure 5: Focus Type III
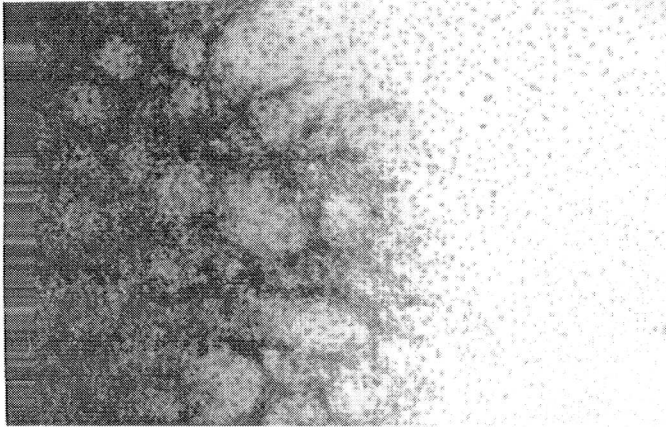
Figure 5 a: Photomicrograph of the edge of a focus type III (25x). Criss-cross patterns are evident of cells growing over the surrounding monolayer.
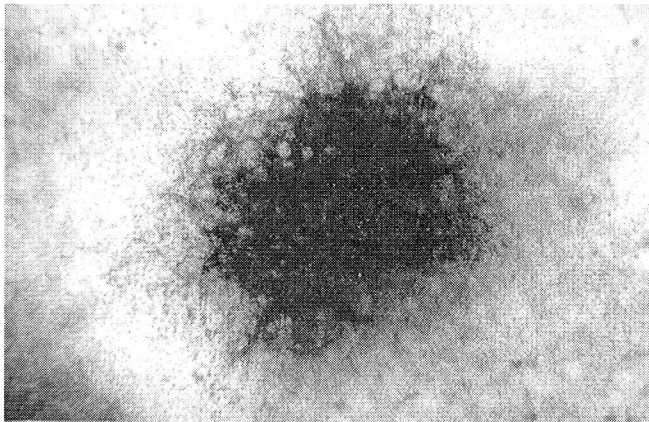
Figure 5b: Photomicrograph of a focus type III (5x). The focus id clearly distingiushed from the background of non-transformed cells. The internal portions of the focus are composed of multiple cell layers.

Figure 6: X-ray Transformation Frequency
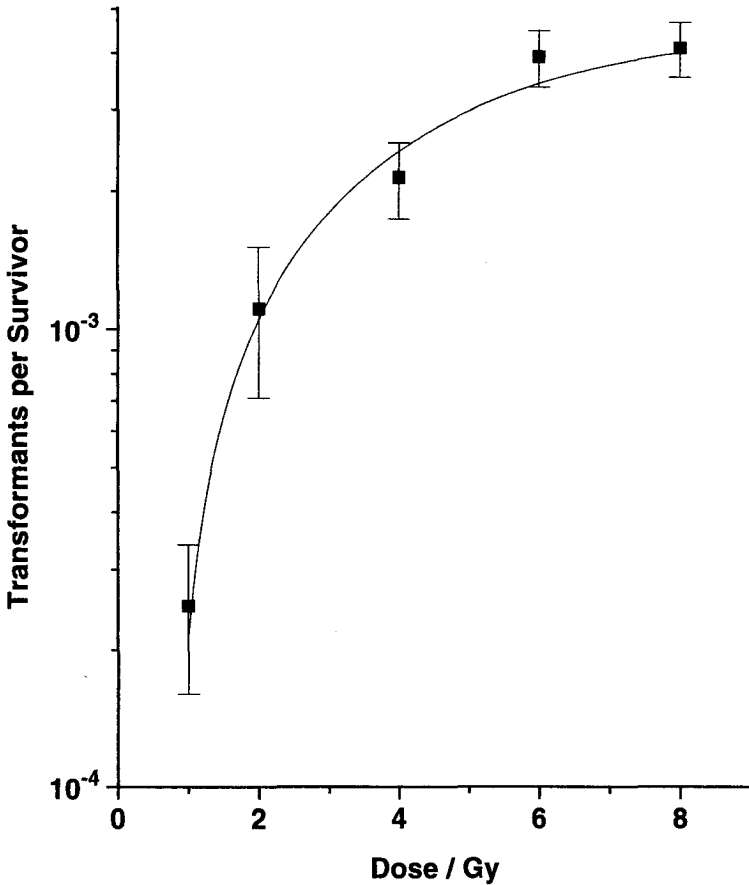
Figure 6: Induced oncogenic transformation per survivor of C3H 10T1/2 cells after high dose rate X-ray (0.9 Gy min^{-1}). The data points shown are pooled results of 4 to 5 independent experiments. Uncertainties are standard errors, for details see materials and methods, 2.2.3. The best fit to the data is a linear-quadratic curve with $\alpha = -0.001 \pm 0.0003$ Gy^{-1} and $\beta = 0.00005 \pm 0.00003$ Gy^{-2}.

2.3. Subcloning of transformed cell lines

See p. 65. C3H 10T1/2 cells passage no. 13 were subjected to transformation by 8 Gy X-ray (standard protocol, see 2.2.3). After 58 and 66 days in culture, distinct type III foci were isolated by ring cloning. The dishes were washed with PBS/CMF, then a small, sterile metal ring was placed around the foci and sealed with silicone. The ring was filled with trypsine-EDTA and the harvested focal cells were transferred into 25 cm^2 cell culture flasks with 5 ml medium. After 8 days, medium was removed, cells were washed with PBS/CMF, cells were trypsinized and all the cells were seeded into 75 cm^2 flasks (p.1). After reaching confluence, cells were harvested (p.2) and diluted into multiwells at a concentration of one cell per well. Growth of the cells in the wells was carefully monitored. The following reasons lead to rejection of the growing clone: more than one cell initially seeded into a well; any irregularity of growth or non-circularity; satellite clones. Clones from the wells were harvested and seeded into 25 cm^2 flasks. Clones exhibiting the same morphology as the parental C3H 10T1/2 cells were discharged. Fig. 7 shows a photographic documentation of the morphology of isolated foci and established clones with their different characteristics.

DNA histograms were measured by flow cytometry of the morphologically most interesting clones and shown in fig. 7, too. One clone which exhibited an extreme polyploidity (Nr. 111-5A) was subjected to a further round of cloning and fourteen subclones of 111-5A were established.

Figure 7:

Photomicrographs and histograms of DNA content of parental cells and clones, established from focus No.11.

7A: Parental C3H 10 T1/2 cells (25x), confluent monolayer, after 66 days in culture. DNA histogram reflects a hypotetraploid state.

7B: Edge of focus number 11 (25x), a focus with distinct characteristics of type III, after 66 days in culture.

7C: Isolated cells from focus 11 (25x), after 7 days in culture. DNA histogram displays multiple G1-peaks.

7D: Established clone (from focus 11) 112-3B (25x), p. 4 after cloning. DNA histogram is hypotetraploid, although cells do not display distinct contact inhibition.

7E: Established clone (from focus 11) 112-3D (25x), p. 4 after cloning. DNA histogram displays an additional minor hypohexaploid cell population.

7F: Established clone (from focus 11) 111-5A (25x), p. 4 after cloning. DNA histogram is highly anomalous, displaying an extreme polyploidity. This clone was subjected to a further round of cloning.

7G: Established subclone (from 111-5A) B-3D (25x), p. 2 after cloning. DNA histogram displays hypotetraploidity.

7H: Established subclone (from 111-5A) A-6D (25x), p. 3 after cloning. DNA histogram is hypooctaploid.

7I: Established subclone (from 111-5A) D-6A (25x), p. 3 after cloning. DNA histogram is highly anomalous, see also fig. 24.

Fig. 7A

Fig. 7B

Fig. 7C

Fig. 7D

#12:/25/A250R001\FL2-A\FL2-Area
CLONE 11 (2-3B), 11.2.92

Fig. 7E

#12:/27/A273R018\FL2-A\DNA-Area
11(2-3D) p14 f6.4.92

Fig. 7F

#11:/25/A259R007\FL2-A\PI-Area
CLONE 11 (1-5A) p7, 20.2.92
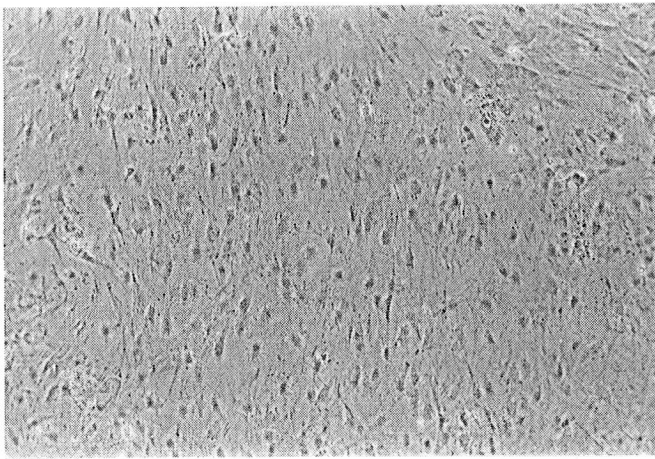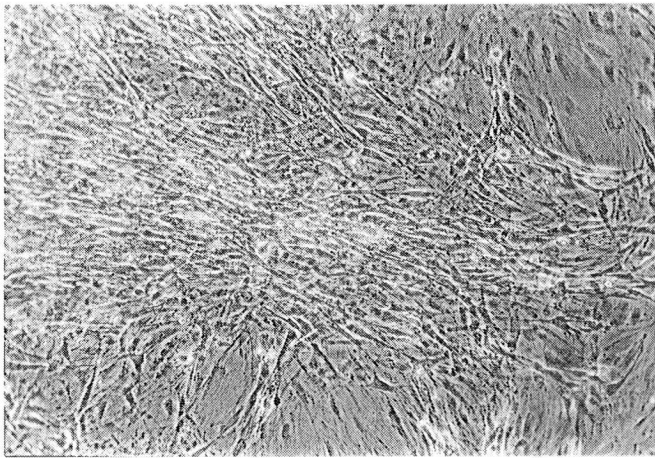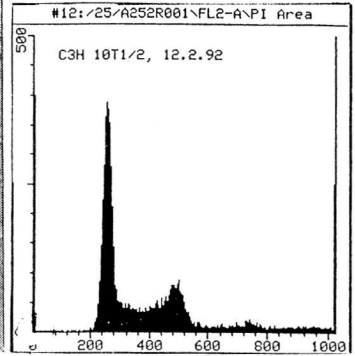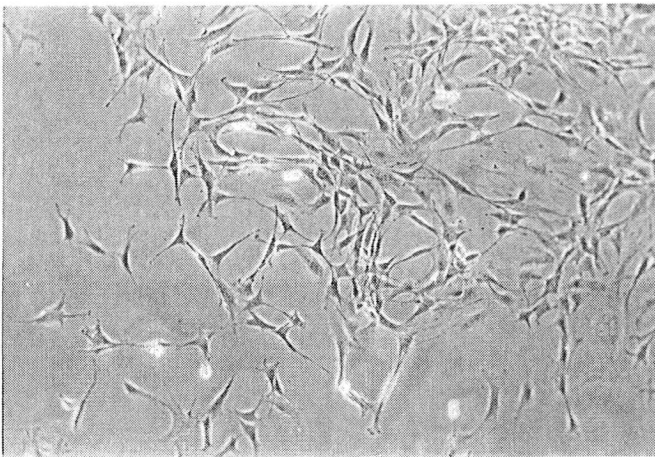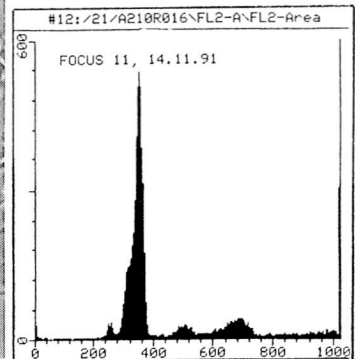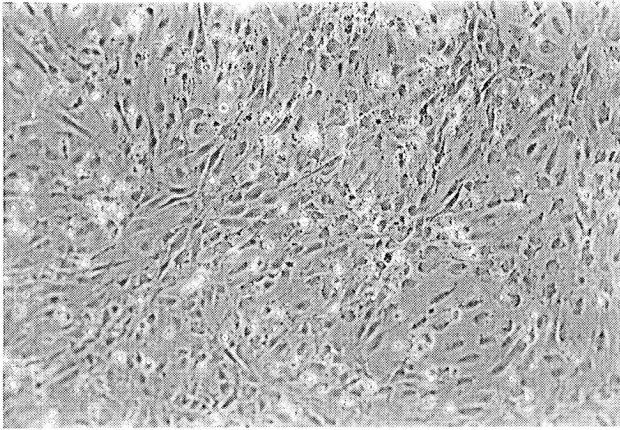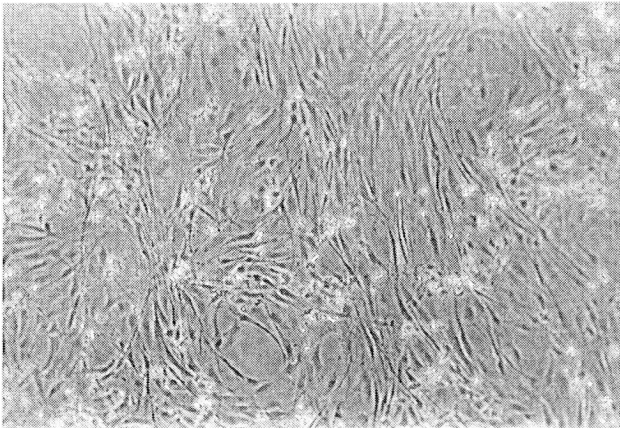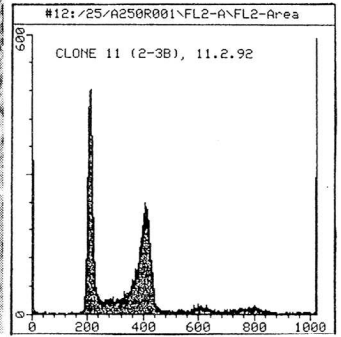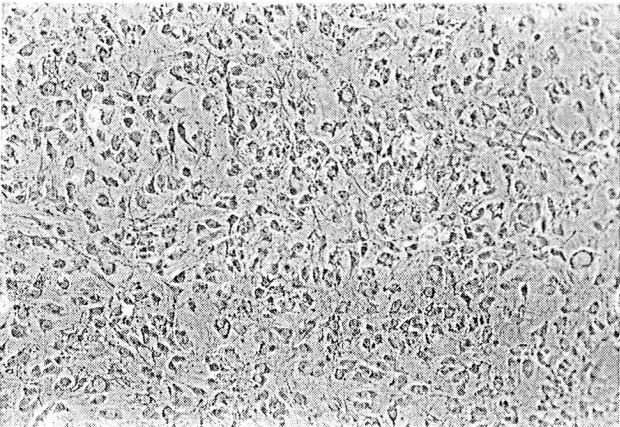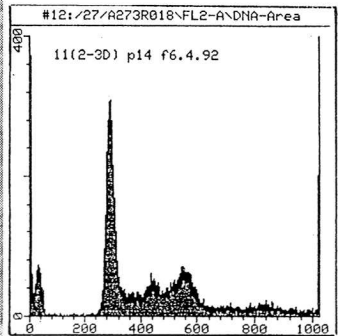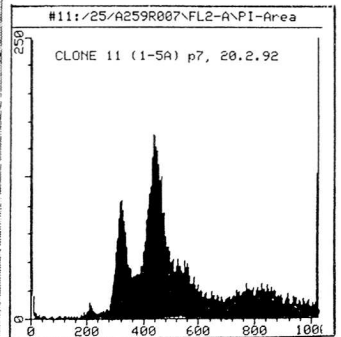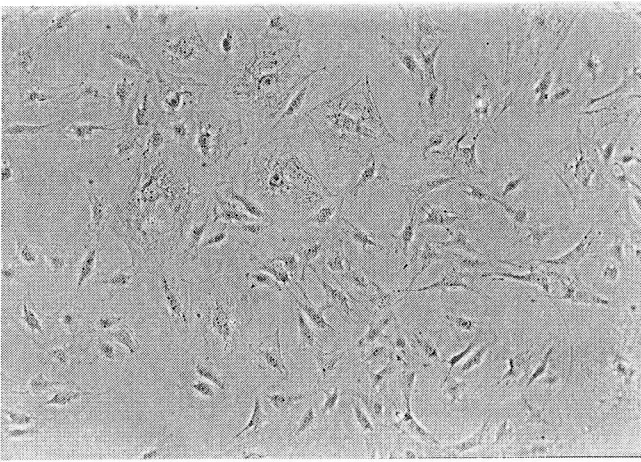
Fig. 7G
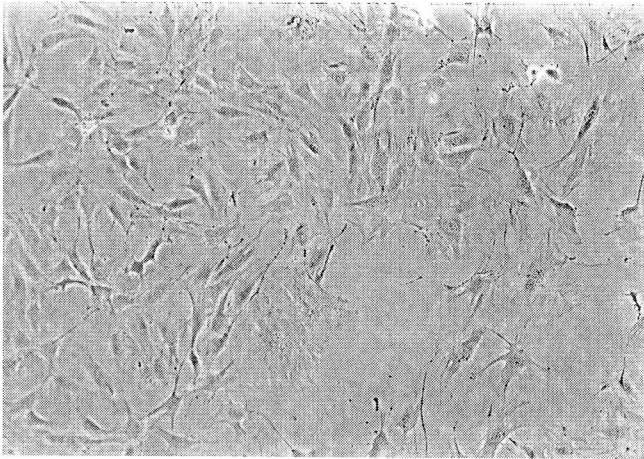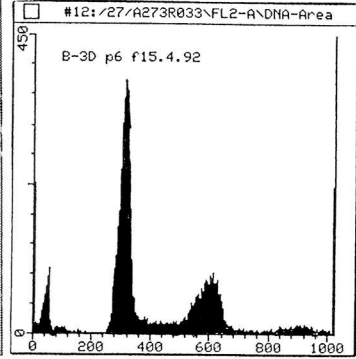
Fig. 7H
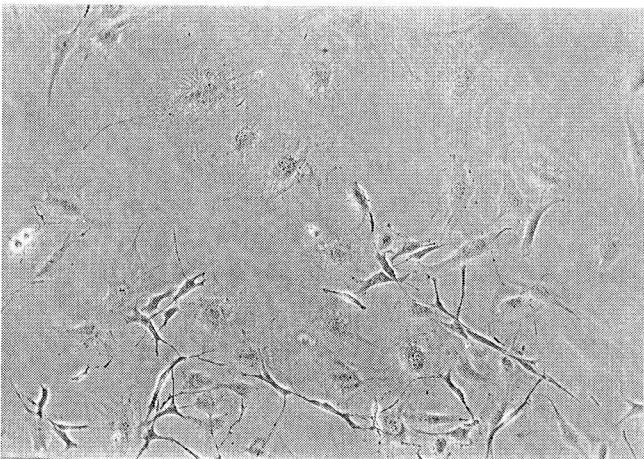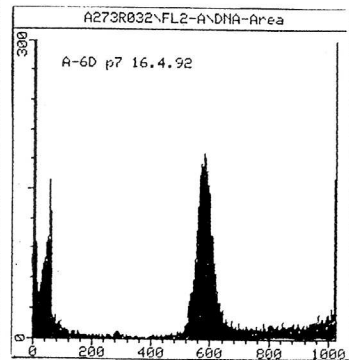
Fig. 7I
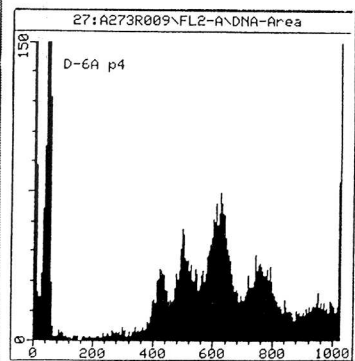
2.4. Inhomogeneous set-up

2.4.1. Yttrium activation

An yttrium metal foil (Johnson Mathey, Cheshire, U.K.) (0.1 x 25 x 25 mm, purity 99.9%) was cut by flame erosion into 0.1 mm thin strips. These narrow Y-89 wires were activated by thermal neutron exposure to a total activity of 1.6 x 10^7 Bq. The activation time t was calculated theoretically [38]:

$$A_B = N_A \cdot \sigma \cdot \Phi \cdot (1 - e^{-\lambda t})$$

Eq. 1

A_B:	Activity at end of activation	=	1.6 x 10^7 Bq.
N_A:	Number of yttrium-atoms		
σ:	Cross section	=	1.28 x 10^{-24} cm^2
Φ:	Neutron flux density	=	3 x 10^{13} n cm^{-2} s^{-1}
λ:	Decay constant $\left(\dfrac{\ln 2}{T\frac{1}{2}}\right)$	=	1.1 x 10^{-2} h^{-1}

2.4.2. Analysis of the activated wire

The activated wires were analyzed semi-quantitatively by γ- and β-spectrometry to quantify the presence of radioactive contaminants. Over 99% of the radioactivity was due to the β-decays from Y-90. The most important contaminating radionuclides were Na-24, Dy-165, Ir-192, Ta-193. Na-24 and Dy-165 were not important for dose estimation, because Na-24 is mainly a γ-emitter and Dy-165 has a short half-time of 2.5 hours. For determination of exact Y-90 activity, a few wires were analyzed quantitatively. After dissolution in diluted nitric acid (1 N) and filtration through two 0.3 μm membrane filters, tantalum and iridium were trapped in the membrane filters (insoluble in diluted acids), but yttrium passed into the filtrate. 200 μl of the filtrate was evaporated and measured in a β-spectrometer. This measured activity never differed more than 10% from the theoretical activity.

5.5 hours after activation the wire was positioned below the basement growth-foil of the culture dishes. At this time point it had an activity of 6 x 10^6 Bq cm^{-1}. During the 24 hours of an experiment, 4.6 x 10^{11} decays per cm took place (mean LET$_\infty$ = 180 eV μm^{-1}, E$_{max}$ = 2.2 MeV).

For dose calculation see p. 33 and p. 47.

For film dosimetry see p. 33.

2.4.3. Cell survival with respect to distance from Y-90 wire

Twenty-four hours prior to exposure the M3-1 cells were plated in special 50 mm culture dishes with a 25 µm thin basement growth-foil (petriperm® dishes, Heraeus, Zurich, Switzerland) at a concentration of 6 x 10^5 cells per dish. subsequently, the Y-90 wire was attached, below the growth-foil, by means of a closely fitting plexi-disc base with a shallow groove for exact placement of the wire. Exposure time was 24 hours in a cell culture incubator.

The method of isolating cells at various distances from the Y-90 wire and subsequent determination of survival is described on p. 36.

2.4.4. Transformation in sublethal dose region

24 hours prior to exposure, cells were plated at a density of 2 x 10^4 cm^{-2} into petriperm dishes. Two different cell culture procedures were performed. Either the cells were plated into the whole petriperm dish or they were plated into agarose trenches only, see fig. 8. When preparing the agarose trenches, two molds (2 x 25 x 5 mm) were placed into a petriperm dish exactly at the position to be investigated (9 mm distance from the future yttrium wire position). Growth medium containing 1% agarose (Serva, Wallisellen, Switzerland) at 60°C was poured into the dishes and left to solidify. The molds were removed and the two resulting trenches washed carefully with PBS to remove any rest agarose.

For each experiment 8 petriperm dishes were irradiated and 4 petriperm dishes were sham-irradiated. For descriptions of the seeding of cells and the isolation of cells after irradiation and their seeding into transformation dishes see p. 54 and p. 57.

2.5. Homogeneous yttrium radiation

2.5.1. Set-up, Dosimetry

For homogeneous yttrium-irradiation, an yttrium foil (0.1 x 25 x 50 mm) was neutron-activated to a total activity of 5.4 x 10^7 Bq (4.4 x 10^6 Bq cm^{-2}). The activated foil was positioned below the basement growth foil by means of a closely fitting plexi disc. Distance between foil and cells was 175 µm.

Figure 8: Frame and Agarose System
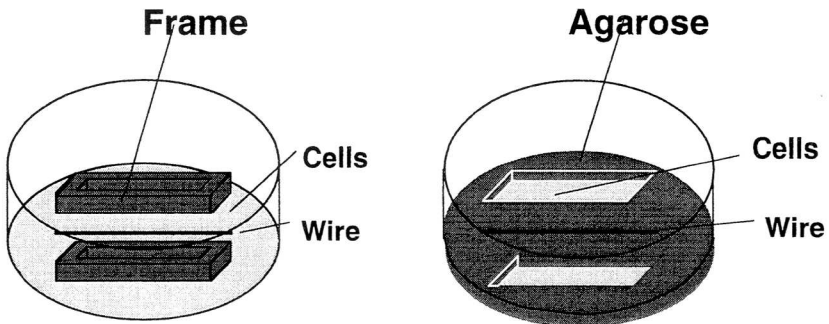
Figure 8: Left side, frame system: Cells were plated into the whole petriperm dish. After irradiation, the wire was removed and two aluminum frames were placed at the defined positions (9 mm distance from the wire). Cells within the frames were trypsinized and isolated.

Right side, agarose system: Agarose dishes were prepared by placing two molds at the defined positions and pouring growth medium containig 1% agarose into the dish. After solidifying the molds were removed and the cells were plated in the resulting trenches.

The duration of exposure was 24 hours. The integrated dose received over this time period was calculated in two different ways:

a) Using the Varskin Mod.2, computer code [39].

b) Using existing estimates of beta-ray dose-rates for plane sources in water [40]

$$\Gamma = 1934 \left[\frac{mGy}{h} \bullet \frac{cm^2}{MBq} \right]$$ *Eq. 2*

Both calculations gave identical doses:

Experiments series 1:   Starting activity: 5.1×10^5 Bq cm^{-2}
                         Dose: 21 Gy (0.88 Gy h^{-1})

Experiments series 2:   Starting activity: 3.1×10^5 Bq cm^{-2}
                         Dose: 13 Gy (0.54 Gy h^{-1})

Experiments series 3:   Starting activity: 1.0×10^5 Bq cm^{-2}
                         Dose: 4.2 Gy (0.18 Gy h^{-1})

Film dosimetry was performed following the same protocol as for the yttrium-wires. The measured doses differed between 10 and 20% from the calculated doses.

2.5.2. Transformation

24 hours prior to the homogeneous Y-90-irradiations, 2×10^5 cells were plated with 2 ml medium in the central area of a petriperm dish. After 1.5 hours 3 ml medium was added. This procedure resulted in the cells settling only in the irradiated area, which was necessary because the active Y-foil had a dimension of 2.5 x 5 cm. Immediately after exposure, cells were trypsinized and diluted into 9 cm dishes at the following concentrations:

21 Gy: Survival: 2000 cells per dish; Transformation: 5500 cells per dish

13 Gy: Survival: 1000 cells per dish; Transformation: 3500 cells per dish

4.2 Gy: Survival: 1000 cells per dish; Transformation: 3000 cells per dish

0 Gy: Survival: 500 cells per dish; Transformation: 1500 cells per dish

3. A PURE BETA LINE SOURCE TO ASSESS HOT PARTICLE EFFECTS *IN VITRO*

M. Sigg, N.E.A. Crompton, and W. Burkart

3.1. Abstract

A model system is presented for assessing the biological effects of inhomogeneous irradiation fields resulting from exposure to particulate radioactive matter (hot particles). The resulting harm per unit dose to tissue is qualitatively different from homogeneous irradiation sources because of specific hot particle effects such as wasting of dose to necrotic tissue (overkill) and formation of microlesions leading to growth stimulation in adjacent tissue. In the case of β-emitters, many of the cells in adjacent tissue receive considerable sublethal doses. To assess the influence of local necrosis and growth stimulation on radiation transformation *in vitro*, a neutron activated short yttrium-90 wire was attached to the bottom foil of a cell culture dish. The system achieves doses of up to 200 Gy per hour directly above the wire, rapidly falling off within a few mm to less than 0.5 Gy per hour. Acute cell death of murine M3-1 cells was observed in the highest dose regions. Colony-forming ability as a function of distance from the wire was investigated. The surviving fraction decreased over several orders of magnitude between 3 and 10 mm from the wire. This report describes the physical characteristics of the model system and subsequent biological survival data for mammalian cell culture. It is a useful and versatile system for modelling inhomogeneous radiation field effects.

3.2. INTRODUCTION

The relative risk from inhaled insoluble particulate radioactivity, so-called hot particles, has been discussed for many years. Uncertainties about the risk arise from difficulties in estimating the spatially non-uniform dose distribution and in evaluating biological response in such inhomogeneous fields. In the sixties and early seventies, Dean and Tamplin predicted a very high probability of tumour induction for lung cells exposed to the extremely inhomogeneous radiation fields from highly radioactive particles [41, 42]. For α-emitting particles this hypothesis could be refuted on theoretical grounds [43], by animal experiments [44], and by epidemiological studies on plutonium workers [45]. In the ICRP publication 30 [46] the responsible editorial commission assumed that for the induction of malignant disease, the hazard of radioactive particles deposited in hot spots in the lung is likely to be less than for the same amount of uniformly distributed nuclides. The major argument behind this reasoning was that α-particles have a typical range of only about 50 μm with a clearly defined cut-off leading to acute cell death or total loss of proliferative capability within most of the irradiated field but insignificant effects outside this area where the dose is practically zero.

A large fraction of the local fallout from Chernobyl consisted of particulate radioactivity but, contrary to previous occupational exposures to α-emitting hot particles, this environmental particulate radioactivity was dominated by β-activity from relatively high burn-up of the reactor fuel [3, 47]. As the dose distribution for β–particles is quite different from alpha-particles, the possibility of enhanced cell transformation arises and requires investigation [8]. Deterministic effects such as microlesions arise around β–emitting hot particles. Surrounding this lethally irradiated zone are cells which receive sublethal doses and stochastic radiation effects such as cell transformation become important. Most of the scant experimental data on the biological effects of β-emitting hot particles have come from studies of murine skin exposures. Charles *et al.* have shown that spatially non-uniform exposure on mouse skin is less carcinogenic than uniform exposure for the same average dose delivered acutely over a period of about 1 hour [48]. Only acute effects on pig skin, such as ulceration, were observed after exposure to β-emitting point-sources and no deterministic late-effects, such as dermal thinning, were observed [49]. Small uranium particles, irradiated with neutrons to a total β-activity of 2 kBq and implanted under the skin of nude mice, induced squamous cell carcinoma in 2 of 32 mice and hyperplasia in 24 of 32 mice [15]. In view of the complex multistage

induction mechanisms proposed for lung cancer, more experimental animal studies and *in vitro* cell-model systems are needed to assess the effect of particulate radioactivity. Especially the co-carcinogenic potential of the complex proliferation and differentiation processes which can occur within the sub-lethally exposed radiation fields surrounding β-emitting point-sources needs to be investigated.

An *in vitro* model system was developed to examine β-emitting hot particle effects on a tissue culture cell system. To enhance the number of irradiated cells and to reduce experimental difficulties, a line source rather than one or multiple point sources was used. Short lengths of yttrium-89 wire were neutron activated producing a strongly inhomogeneous radioactive field-source compatible for use with mammalian cell culture. Clonogenicity of the cells in relation to distance from the β-source was determined. The design, dosimetry and cell survival characteristics of this *in vitro* cell-model system are described here.

3.3. Materials and methods

3.3.1. Cells:

M3-1 cells (originally supplied by Dr. M.R. Raju, National Laboratory, Univ. of California, Los Alamos), Chinese hamster bone-marrow cells, were grown in MEM-α (Gibco, Basel, Switzerland), supplemented with 10% foetal bovine serum (Seromed, Bad Zurzach, Switzerland), penicillin (25 units ml^{-1}) and streptomycin (25 μg ml^{-1}). Cultures were kept in a humidified atmosphere of 95% air, 5% CO_2 at 37°C. 24 hours prior to exposure the cells were plated in special 50 mm tissue culture dishes with a 25 μm thin basement growth-foil (Heraeus, Zurich, Switzerland) at a concentration of 6 x 10^5 cells per dish. During irradiation the cells were in exponential growth.

3.3.2 Irradiation:

An inactive yttrium foil (Johnson Matthey, Cheshire, U.K.) (0.1 x 25 x 25 mm, purity 99.9%) was cut by flame erosion into 0.1 mm thin filaments (Fig. 9). These Y-89 wires were activated by thermal neutrons ($\Theta = 3$ x 10^{13}n cm^{-2} sec^{-1}) to an activity of 1.6 x 10^7 Bq per wire.

Figure 9: Yttrium Wire
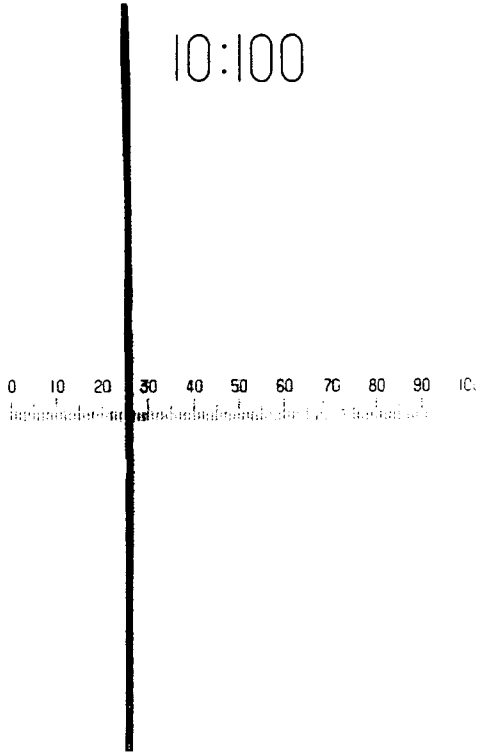
Figure 9: Micrograph of an yttrium wire. One unit on the micrometer corresponds to 100 µm, therefore, total length is 1 cm.

The activated wires were analysed by γ- and β-spectrometry. Over 99 % of the radioactivity was due to the β-decays of Y-90. Minor contamination came from sodium-24, dysprosium-165, iridium-192, tantalum-193 and yttrium-91.

The wire was attached below the basement growth-foil of the culture dish by means of a closely fitting plexi-disc with a shallow groove to fix the position of the wire. Exposure time was 24 hours starting at 5.5 hours after activation.

3.3.3 Dosimetry:

For dosimetry calculations the Y-90 wire was regarded as a line source [50] with a half-life of 64.1 h and a mean LET of 180 eV μm^{-1} [51]. The physical dimensions and self-absorption effects of the yttrium wire were neglected.

The particle flux density ϕ of a line source is:

$$\phi = \frac{S_L}{4\pi a} \cdot (\theta_1 + \theta_2) \qquad (Eq.\ 3)$$

S_L:specific strength of line source; for other parameters see fig. 10.

After solving for θ_1 and θ_2 the function

$$\frac{a \cdot L}{a^2 - d \cdot L + d^2} = \left(\frac{\phi \cdot 4\pi a}{S_L} \right) \qquad (Eq.\ 4)$$

was numerically solved and integrated over 24 h and along the wire

$$(\int_0^{24} S_L = 4.9 * 10^{11} cm^{-1}).$$

The dose D was:

$$D = \frac{LET \cdot \phi}{\rho} \qquad (Eq.\ 5)$$

with $\rho = 1$ g cm^{-3}.

An alternative method to determine dosimetry was performed using Varskin Mod2, a computer code for assessing dose from skin contamination [39]. This code is based on Berger's formula and takes the β-spectrum into account.

For dosimetry measurements a film (X-OMAT V, Kodak, Lausanne Switzerland) was exposed to the radioactive wire, developed (Gevamatic 60, Agfa, Duebendorf, Switzerland) and densitometrically analyzed by a laser scanner (BioImage, Millipore, Volketswil, Switzerland; 1 pixel = 84 μm).

Strontium-90/Yttrium-90 was used as a reference source (NPL secondary standard for beta-ray protection level dose-rates), see fig. 11.

The X-OMAT V is a double coated film. The thickness of the film and the resultant differential darkening of the two sides were included in the

Figure 10: Geometrical Basis for ϕ
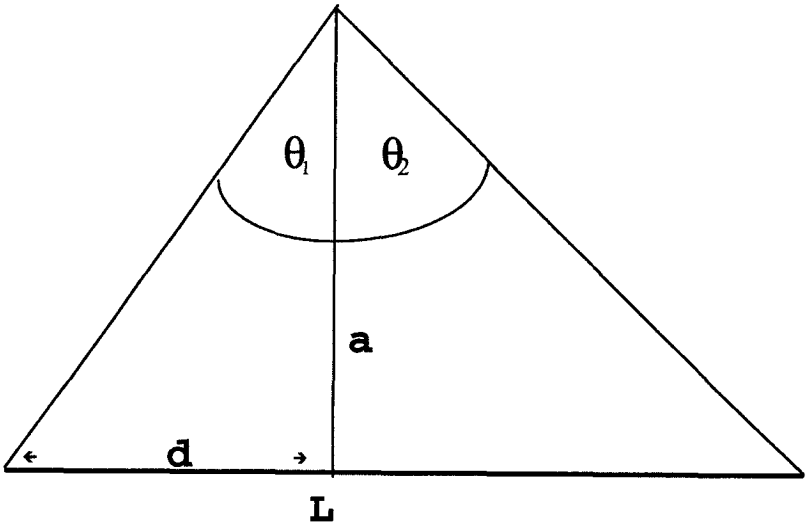
Figure 10: Geometrical basis for calculation of the particle flux density ϕ [50]. Details of calculations are given in the materials and methods section.

a: shortest distance to line source from measured point. Determined on surface of dish but taken into consideration depth of wire below dish surface. L: Line source = 25 mm.

Figure 11: Calibration Curve
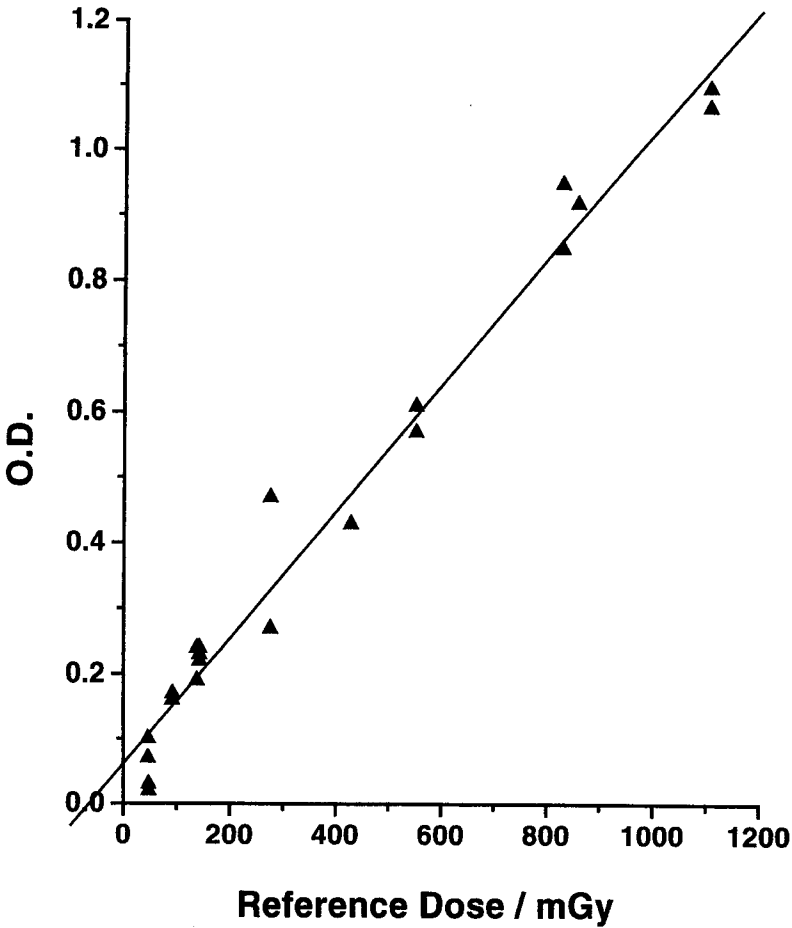
Figure 11: Calibration curve for film dosimetry. Optical density *versus* reference dose [mGy]. Reference source was a NPL secondary standard for beta-ray protection level dose-rates, Sr-90 + Y-90. Absorbed dose-rate to tissue 7.0 mg cm^{-2} = 13.79 ± 3.4 mGy h^{-1} (21 June 1985).
O.D. = 0.06 + 9.67 E-4 * Dose; r = 0.988 .

calculations. Only measurements in the linear region (dose versus blackness) were made. Linearity was confirmed by a control-sequence of X-ray exposures.

3.3.4 Survival assay:

Cells were grown in Petri dishes on a thin basement growth-foil which could be placed over the source. Following exposure, the dish was transferred from the plexi disc with the yttrium wire to an equivalent plexi disc engraved with a cutting stencil. Care was taken to ensure the orientation of the growth foils was exact. The cells were washed with CMF-PBS and the basement growth-foil was cut into small strips with a sterile scalpel (see fig. 12 for cutting pattern). The cells on these strips were subsequently removed by trypsinization (Trypsin-EDTA, Gibco, Switzerland) and plated into 90 mm culture dishes according to the following concentrations: All cells from strip 9 were plated into a single dish, those from strips 7 and 8 into three dishes and those from strips 5 and 6 into five dishes. The cells from strips 1, 2 and 3 were plated into five dishes after pre-diluting 600-fold. Cells from the foil periphery, 10, were counted and diluted to give a final concentration 300 cells per dish. A control dish with the same density of non-irradiated cells was treated in exactly the same manner.

After five days the colonies were washed with 0.9% saline, fixed with methanol/glacial acetic acid (3:1 v/v) and stained with crystal violet (10 g in 1 l methanol). Colonies with more than 50 cells were scored as survivors. To obviate problems associated with irregularity in cutting of the growth-foil, colony yield was determined per weight of growth-foil. During the course of these experiments 255 strips of 1 mm width were cut and weighted. The average weight was 1.54 mg with 10% deviation. Estimates of the effect of this error on exposure dose revealed an insignificant effect at distances from the wire greater than 2 mm. Surviving fraction was expressed as the ratio of irradiated colonies to non-irradiated control colonies, which included corrections for plating efficiency.

Figure 12: Cutting Pattern
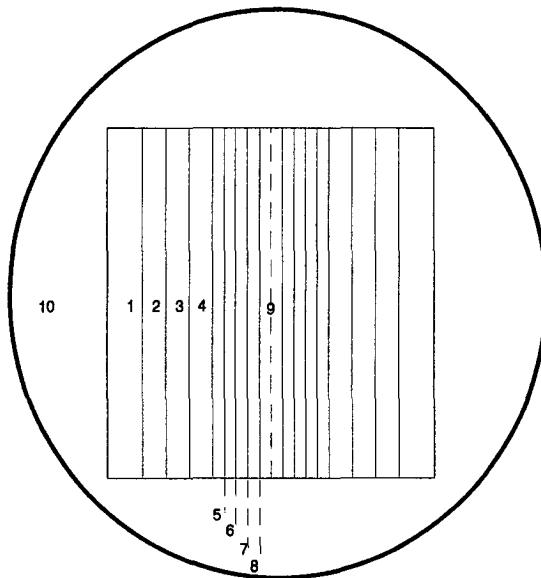
Figure 12: Cutting pattern of growth-foil. After irradiation the growth-foil was dissected with a scalpel. Central dashed line: previous position of yttrium wire. Strips 5 - 8: 1 mm x 25 mm; strips 9 and 2 - 4: 2 mm x 25 mm; strip 1: 3 mm x 25 mm; area 10: rest of the basement growth-foil of the 5 cm dish. For strips 1 - 8, cells on both sides of the wire were pooled.

3.4. Results

3.4.1 Dosimetry:

The estimated dose of the Y-90 wire-source, integrated over 24 hours and along the length of the wire (*Eq. 5*), was 5'570 Gy directly above the wire, 380 Gy at 1 mm distance, 20 Gy at 10 mm distance and 5 Gy at 25 mm distance (*i.e.,* the edge of the dish), see fig. 13. Fig. 14 compares the estimated dose integrated over 24 hours with the Varskin dose but only at points equatorial to the wire. There was no integration along the length of the wire.

Fig. 15 shows the means and standard errors of the dosimetry measurements compared with the estimated dose for each single pixel and the Varskin dose. The measured dose-curve had a slightly different shape than the estimated curve. In the highest dose regions it was about 30% higher.

3.4.2 Survival assay:

After 24 hours of irradiation, cell loss and necrosis were observed near the wire-source. The most extensive region of necrosis was observed in the immediate vicinity of the wire. Cell survival as a function of dose (distance from wire) was determined quantitatively and reflected the extremely steep decrease in dose distribution determined by the dosimetry (see fig. 16). Approaching the wire from the edge of the dish revealed only a small decline in survival, up to 8 mm distance. The survival within this region was consistently greater than 0.7. At closer distances a steep decrease occurred, over several orders of magnitude, down to 0.001 at about 4 mm distance (70 Gy total dose). In the very high dose region the curve flattened to a minimum plateau.

Fig. 17 displays the dose-response curve. Error bars indicate standard error for 17 independent experiments. Up to 100 Gy total dose the data best fit a

multitarget, single hit model of the form $S = \left(e^{-D/_1D_0} \right) * \left\{ 1 - \left(1 - e^{-D/_1D_0} \right)^n \right\}$

(*Eq. 6*). The best fit parameters are $n = 25$, $_1D_0 = 140 \pm 40$ Gy, and $_nD_0 = 8.8 \pm 0.4$ Gy [52]. The linear quadratic model gives a negative value for $\alpha = -0.009 \pm 0.005$ Gy^{-1}, and $\beta = 0.001 \pm 0.0002$ Gy^{-2}. The poor fit is due to the continuously bending form of the model in the high dose region. The plating efficiency was 84.6 ± 1.91 (n=17).

Figure 13: Estimated Dose
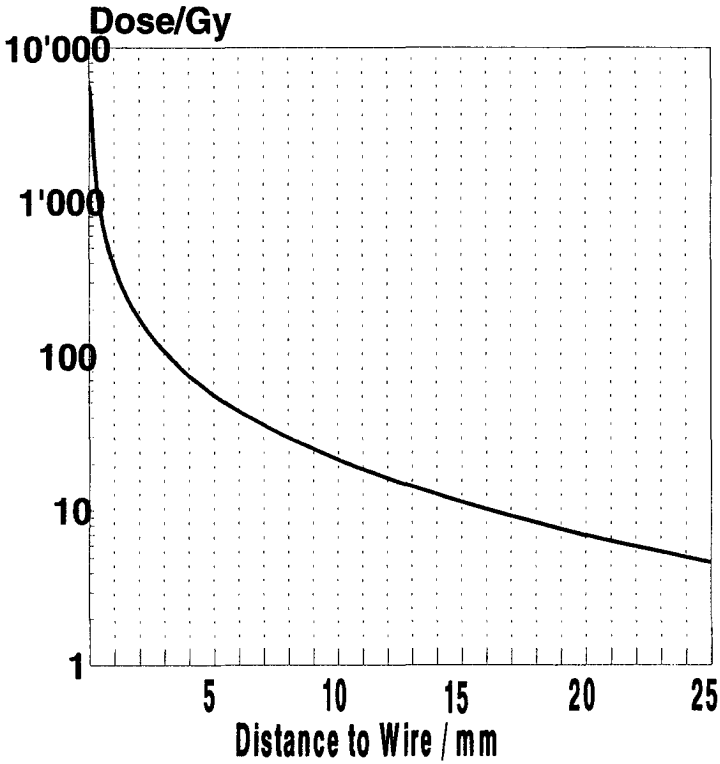
Fig. 13: Estimated dose, calculated from equation 5. Dose was integrated over 24 hours and along the wire and based on integrated activity of yttrium line source: 4.9×10^{11} cm^{-1}. The "distance to wire" is a measure of the distance to a point immediately above the wire along the surface of the basement growth-foil.

Figure 14: Estimated and Varskin Dose
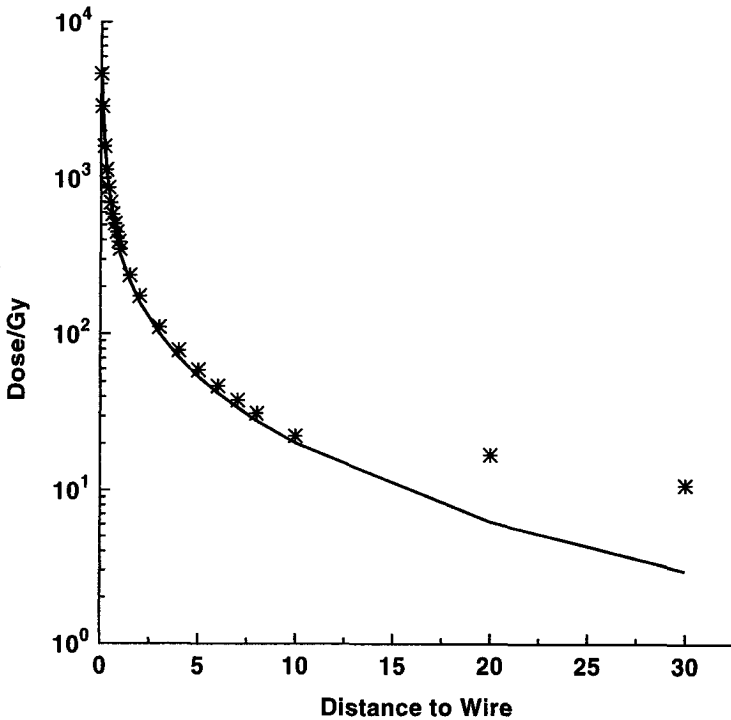
Figure 14: Comparison of the estimated dose and the Varskin dose. The estimated dose (continuous line) was determined using equation 5 described in the materials and methods section. The Varskin dose was determined using the VARSKIN MOD2 code (stars). Total activity of the wire: 4.9×10^{11} cm^{-1}. Dose was integrated over 24 hours but only at points equatorial to the wire. There was no integration along the length of the wire. The "distance to wire" is a measure of the distance to a point immediately above the wire along the surface of the basement growth-foil.

Figure 15: Measured Dose
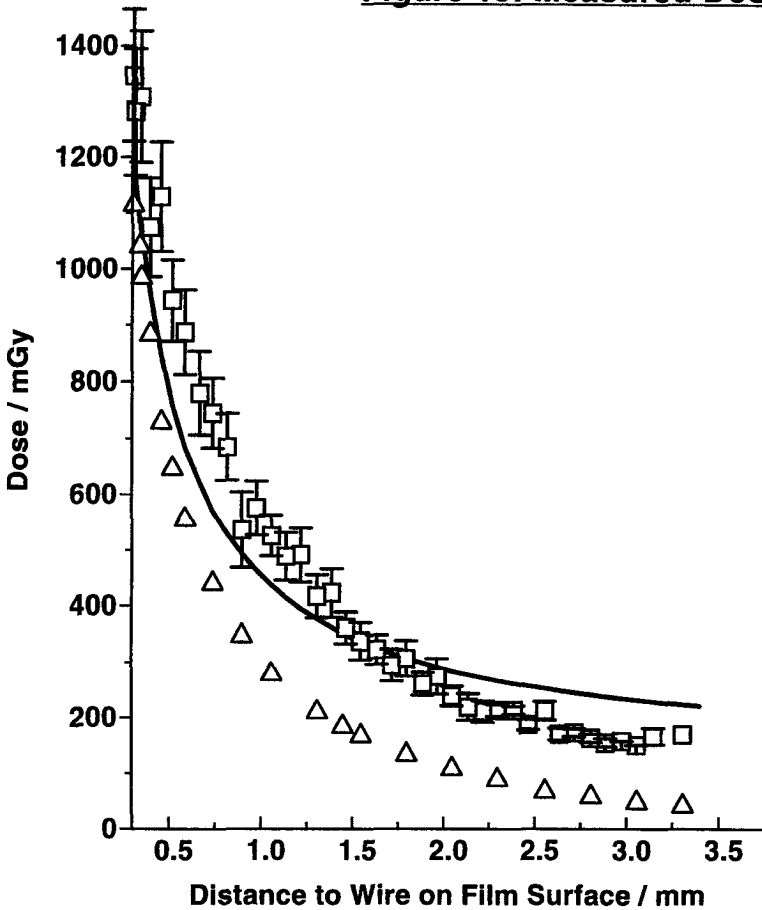
Figure 15: Measured dose. Mean and standard error of dosimetric measurements from 5 independent experiments. Activity of line source: 4.6 x 10^8 cm^{-1}. The continuous line is the estimated dose for one side of the radiation field, triangles are the dose calculated by VARSKIN MOD2. Error bars are only marked if they were bigger than the symbol. The "distance to wire on film surface" is a measure of the distance to a point immediately above the wire along the surface of the dosimetry film.

Figure 16: Dose and Survival
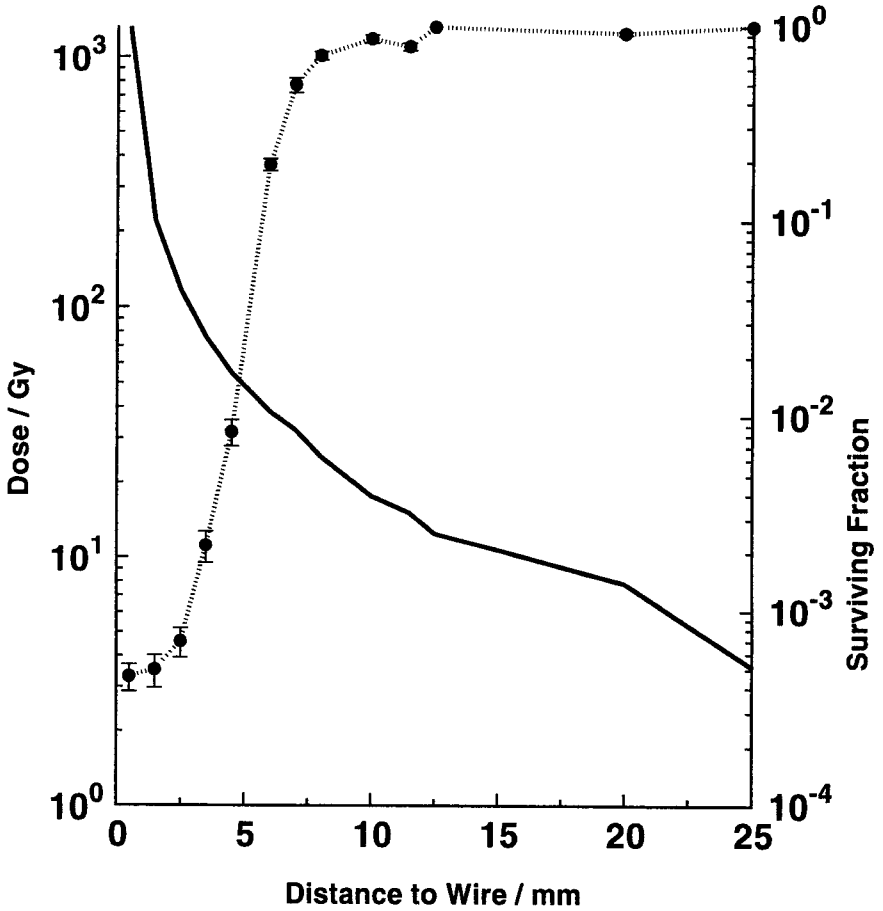
Figure 16: Dose and survival as a function of distance from Y-90 wire source. Solid line: dose (integrated over area of strips); Dotted line: Surviving fraction at specific distances (points joined for clarity). Error bars mean standard error of 17 independent experiments.
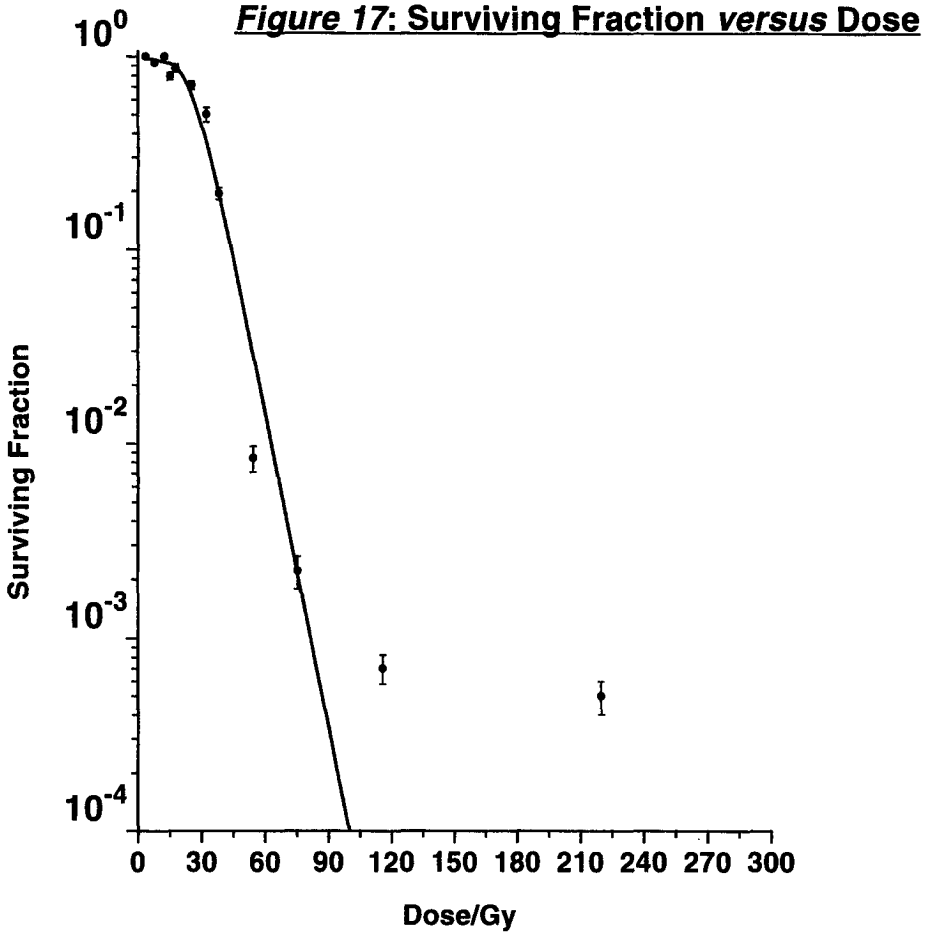
Figure 17: Surviving fraction *versus* dose (integrated over area of strips). Error bars are standard errors of the means of 17 replicate experiments. The fitted line is a best fit multitarget, single hit curve. For details see text.

3.5. Discussion

A model system has been developed to assess β-emitting hot-particle effects on a mammalian tissue culture cell system. Hot particles can be compared to a radiation point-source. However, the use of a line source provided many advantages: the inhomogeneity of the radiation field is similar, more cells are exposed, and high numbers of equally damaged cells are equi-distant from the source.

Yttrium-90 was chosen as a radiation source for the following reasons: it emits pure, high energy electrons; as a foil or as wires of yttrium-89 it is readily manipulated and compatible with cell culture limitations; and it has a reasonably high neutron cross-section. After neutron activation little γ- contamination was detected which was only inconvenient with respect to radiation protection requirements and did not interfere with the experiment itself. The short half-life of 64 hours did not permit irradiation with a constant dose rate. At the end of a 24 hour experiment the dose rate was 76% lower than the initial level which is why the results are only expressed as "total" doses. However the decline during the experiments is not considered critical for most tests envisaged. Since the exact dimensions of the wire are a critical parameter for dose estimations, care was given to produce wires with as less variations as possible as demonstrated in fig. 9.

For dose calculations an average LET for the Y-90 β-particles of 180 eV μm^{-1} was used. Because this value may not be correct for all dose regions since the energy differs at various distances, we also performed a Varskin dose determination. Out to distances of more than 1 cm the estimated dose and the Varskin dose were equivalent. At greater distances the two doses diverged. Dose effects at source edges have been discussed by Prestwich *et al.* [53]. Film dosimetry was performed to confirm the dose estimates. The errors observed result from several experimental difficulties. First, the exact activity of every wire could not be determined exactly as this required dissolution of the wire; expected variation is about 10%. Second, the film scanner measured the absorption in pixels of 84 μm size; repeat measurements of the same area displayed an inter-measurement variation of about 5%. Third, film development conditions (temperature, time, chemicals) were not vigorously controlled; expected variation is about 10%. The experimental dose curve had a slightly different shape than the estimated curve. In the high-dose region the experimental curve was about 20% higher than the estimated curve and the greatest errors were also observed here. On average, the calculated dose

fluctuated from the measured film value by less than 20% which appears to confirm the validity of the model system and the estimates of dose. Although the choice of a double sided-film for dosimetry purposes could be improved upon, the system appears suitable for investigation of biological effects.

A strong dose-rate effect was observed with the colony-forming assay. The colony-forming ability in the shoulder region (from 3 to 30 Gy in 24 hours) was higher than otherwise reported in the literature for low dose-rate experiments [54, 55, 56]. Three important factors influence the dose-rate effect; the quality of the ionising radiation, the cell-cycle stage during irradiation and sublethal damage repair. Few studies have examined the radiobiology of exponentially decaying irradiation. Wong compared irradiation with Y-90 labelled antibodies (initial dose rate 0.25 to 2.9 Gy h^{-1}, exposure time 21 days) to irradiation with Co-60 (1.6 Gy min^{-1})external beam irradiation on two human colon carcinoma cell lines and found colony formation after Y-90 exposure to be less effective by a factor of 2.4 to 3.4 [57].

A complex picture of proliferation and repair during Y-90 irradiation was observed in the cell cultures. Proliferation is usually possible only at low-dose rates, in our system these conditions existed only at the edge of the dish. Because surviving fraction is expressed as the ratio of irradiated colonies to non-irradiated control-colonies, the effects of both induction and inhibition of proliferation during irradiation are reflected in the resulting survival data.

Due to the extremely inhomogeneous radiation field, cells with different degrees of damage were in close association. This could enhance or reduce biological responses (e.g. repair, or proliferation and transformation) important in the *in vivo* situation.

The flattening of the survival curve may simply be an artefact caused by the dissection of the basement growth-foil when cross-contamination of poorly attached cells from sublethally irradiated regions may have occurred.

The survival curve could be fitted by a multitarget, single hit model up to total doses of 100 Gy. The fitted parameters, however, cannot be compared with others reported because in the heterogeneous dose situation dose-rates differ with distance from the source and, furthermore, decrease exponentially during the course of the experiment. D_0 was for high dose-rate X-ray survival assays 2 Gy (M3-1 cells, data from our laboratory), $_1D_0$ was 18.2 Gy (CHO cells, Elkind 1977). $_1D_0$ was therefore by a factor of 7.7 lower than in this heterogeneous beta irradiation system.

An approach to the problem of simulating an inhomogeneous radiation field surrounding a β-emitting hot particle is described. In a cell culture dish

conditions can be produced where regions of markedly different levels of damage exist in close proximity; from "supralethality" (interphase death directly above the wire) to sublethality. This reflects an important feature of β-emitting hot-particle exposures. The zone of sublethal dose exposure is particularly pertinent with respect to investigations of radiation-induced transformation. Using C3H 10T1/2 cells as tissue culture system will allow to study transformation effects in an extremely inhomogeneous radiation field. Assessment of hot particle effects *in vivo* is complex due to the dynamics of the affected tissue and to associated non-stochastic biological effects. With this *in vitro* cell-model system we have a tool to investigate critical aspects of transformation, growth stimuli or cell-cell communication in an inhomogeneous β-radiation field which should help reduce the uncertainties associated with prediction of risk from the biological effects of inhaled particulate radioactivity.

4. CORRECTION OF DOSIMETRY

A revised interpretation of the dose estimations indicated some discrepancies, therefore, an exact re-evaluation of all assumptions and calculations pertaining to the Y-wire dosimetry was performed.

All previous dosimetric calculations were based on the assumption of a dimensionless line source. For exact alignment, the yttrium wire was placed in a groove, which was 200 μm deep. Due to this geometric situation, part of the β-particles passed through plexiglas and were absorbed. This absorption had been neglected in the previous calculations. It was dependent on the distance through the plexiglas and, therefore, dependent on the angle between the wire and exposure point. A small air gap between the plexiglas and the basement foil of the culture dish had a significant influence under these circumstances, because it reduced the effective distance passed in plexiglas.

The air gap was determined with an exact slide calliper, and was the difference between the distances from the edge of the culture dish to the bottom of the culture dish and from the edge of the culture dish to the surface of the plexi disc.

The film dosimetry presented in the Health Physics paper is correct, because it was performed without the plexiglas-groove and air gap. The wire was directly positioned onto the covering paper of the dosimetric film and weighted with plexiglas. However, the estimated dose distributions were incorrect.

The revised dosimetric approach is based on the Berger point kernel [58]:

$$B(r) \quad = \quad k\, E_\beta\, Y\, F_\beta\, (r_1 / X_{90}) / (4\pi\, \rho\, r^2\, X_{90}) \qquad \textit{Eq. 7}$$

$$D \quad = \quad B(r) \cdot 1.15 \cdot 10^{12} \qquad \textit{Eq. 8}$$

$B(r)$ = Berger point kernel $(Gy\ s^{-1}\ decay^{-1})$

r = a variable representing the distance between a source point and a dose point

k = a unit conversion standard

E_β = the average beta energy (= 0.95 MeV)

Y = the beta yield per disintegration (= 1)

$F_\beta\,(r_1 / X_{90})$ = the scaled absorbed dose distribution as a function of the modified path length and the X_{90} distance, calculated by the computer code SADDE Mod 2 [39]

r_1 = the modified path length between the source point and dose point (= $r\, \rho$)

ρ = the density of the irradiated medium (1 for tissue, 0.0013 for air, 1.16 for plexiglas) $(g\ cm^{-3})$

X_{90} =   radius of a sphere in which 90% of the beta energy is deposited from a point source in an infinite medium

D   =   dose   (Gy)

$1.15 \cdot 10^{12}$ =   total number of decays for 24 hours of an yttrium wire with a starting activity of $1.5 \cdot 10^{7}$ Bq

The term $E_\beta \cdot F_\beta$ corresponds to dE / dx which refers to the energy deposited per distance. The dose was numerically integrated along the wire, by dividing the length in small pieces and calculating for each target point the dose contribution of each piece. A limited backscatter correction is incorporated into the Berger point kernel, since the original calculations assume an infinite water medium. For the geometric situation with a thin wire, an air gap and a plexiglas background, backscatter would be overestimated. Therefore, correction for backscatter was made by dividing the kernel by 1.3 (= backscatter correction factor [59]).

The revised dose distribution results in an overall reduction in dose. The decrease in dose with distance from the wire is extremely steep, the irradiation field over the whole dish is inhomogeneous. The dose, integrated over 24 hours and along the wire directly above the wire is 750 Gy and decreases rapidly to 10 Gy at about 8 mm distance, 1 Gy at 14 mm distance and zero at 21 mm distance from the wire, fig. 18. Dose and surviving fraction as a function of distance from the wire are presented in fig. 19. Fig. 20 shows the best fit for the survival data. It is a linear quadratic function with $\alpha = 0.014 \pm 0.00024$ Gy^{-1} and $\beta = 0.0038 \pm 0.00004$ Gy^{-2}.

The revised dosimetry better accounts for the extremely steep decrease in survival observed, but has no direct influence on the basis for the transformation experiments. The ideal sublethal dose region for the transformation assays was based on measured survival data. This region, between 9 and 11 mm distance from the wire, displays a constant cytotoxicity. The dose, numerically integrated over this area, is 6 Gy, administered at a dose-rate of 4 mGy min^{-1}.

Figure 18: Estimated Dose
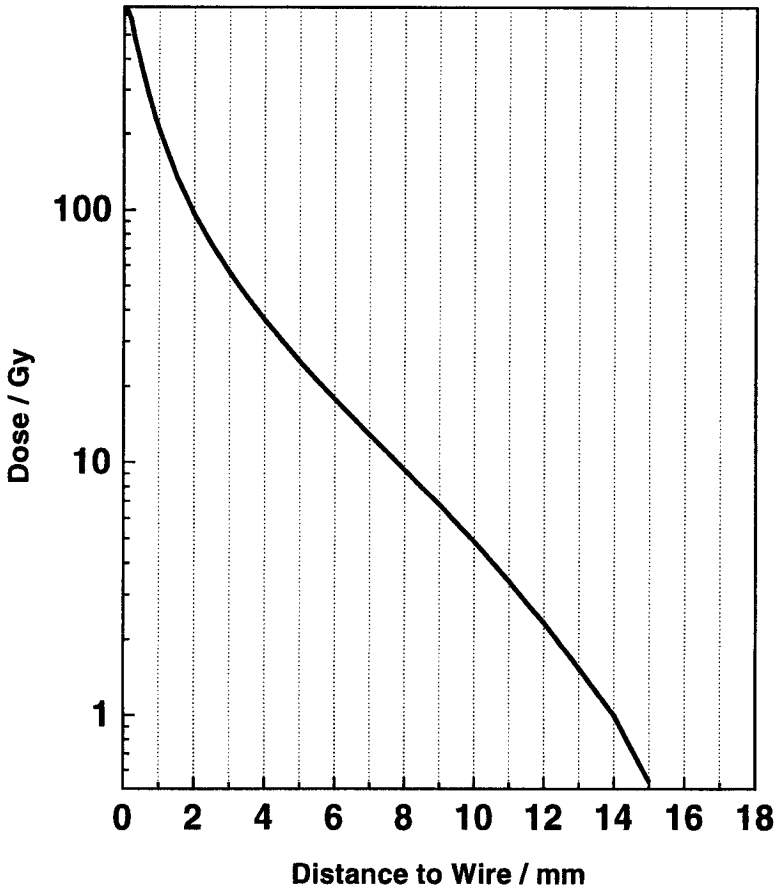
Figure 18: Estimated dose, calculated from equation 7. Dose was integrated over 24 hours and along the wire and based on integrated activity of yttrium line source: 4.9×10^{11} cm^{-1}. The "distance to wire" is a measure of the distance to a point immediately above the wire along the surface of the basement growth-foil.

Figure 19: Dose and Survival
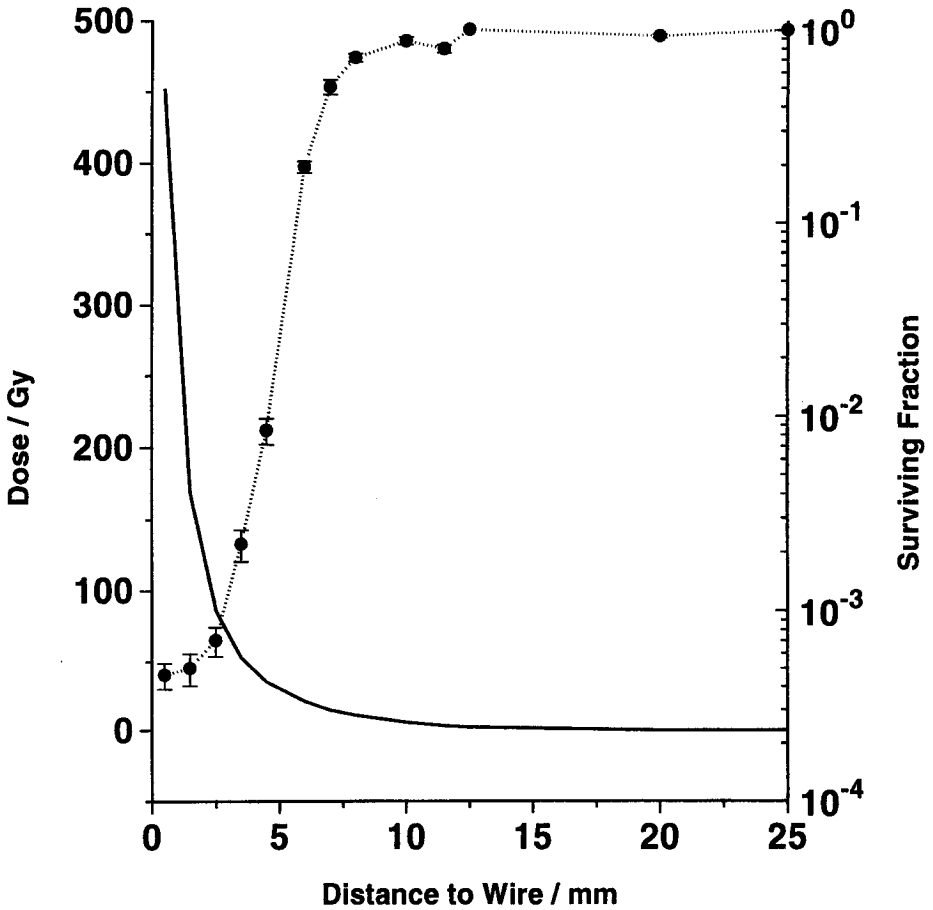
Figure 19: Dose and survival as a function of distance from Y-90 wire source. Solid line: dose (integrated over area of strips); Dotted line: Surviving fraction at specific distances (points joined for clarity). Error bars mean standard error of 17 independent experiments.
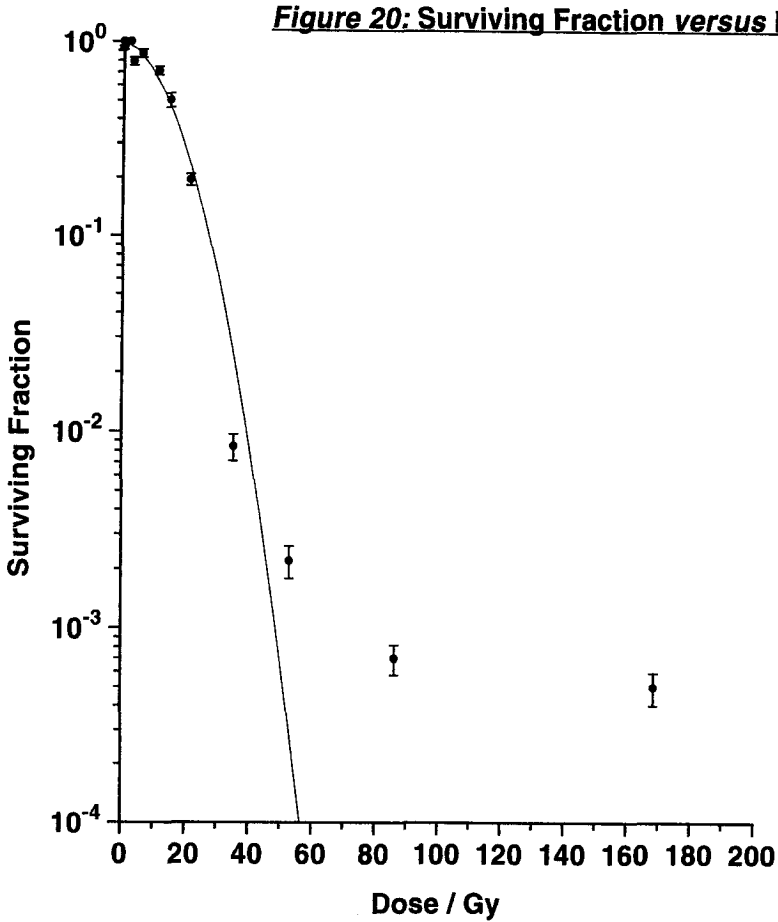
Figure 20: Surviving fraction *versus* dose (integrated over area of strips). Error bars are standard errors of the means of 17 replicate experiments. The fitted line is a best fit multitarget, single hit curve with $\alpha = 0.014 \pm 0.00024$ Gy^{-1} and $\beta = 0.0037 \pm 0.00004$ Gy^{-2}.

5. ENHANCED TRANSFORMATION IN AN INHOMO-GENEOUS RADIATION FIELD: AN EFFECT OF THE PRESENCE OF HEAVILY DAMAGED CELLS

Martina Sigg, Nigel E. A. Crompton, and Werner Burkart[2]

5.1. *Abstract*

In the inhomogeneous radiation field surrounding small beta-sources, non-lethally and heavily damaged cells are in close proximity permitting interaction via extracellular signals. This situation is typical of hot particles such as those released from Chernobyl. Beta-emitting yttrium-90 wires were employed to investigate radiation-induced cell transformation under these conditions. Integrated 24 hour-doses ranging from 750 Gy to zero Gy across the exposure field were applied. At equal levels of toxicity a ten-fold enhancement of transformation frequency in C3H 10T1/2 cells was observed in the presence of heavily damaged cells. Homogeneous fields of low dose-rate beta-irradiation produced transformation frequencies typical for comparable photon exposures reported in the literature.

5.2. *Introduction*

After the reactor accident at Chernobyl, hot particles, i.e. highly radioactive particles made up of fission- and activation products, were deposited throughout Europe. Radiation exposure from hot particles poses a problem, which cannot be assessed properly with the dosimetric models currently employed in health physics (for review see [8]). Once deposited (e.g. within the lung), an extremely inhomogeneous radiation exposure is caused by these hot particles. Dose rates and total doses vary from ultra high to low within a few cell diameters, and non-lethally damaged cells are within chemical signalling range of superlethally irradiated and heavily damaged cells, especially in the case of β-hot-particles due to their continuous energy spectra. A number of reports document that cells not traversed by an α-particle but within an α-radiation field and, therefore, in the presence of heavily damaged cells, display enhanced frequencies of sister chromatid exchanges and enhanced induction of p53 expression [60, 61, 62].

Servomaa *et al.* [63] added isolated β-hot-particles directly to a monolayer of C3H 10T1/2 cells and observed an extremely enhanced transformation rate. All foci were within 2 - 4 mm of the radiation source. Death of the surrounding cells and an enhanced mitotic activity of cells around the lethal zone were also observed. In the same laboratory β-hot-particles were also implanted under the skin of nude mice and, subsequently, epidermal tumours were observed in excess of estimates from the conventional non-threshold stochastic model of radiation-induced cancer [15]. The aim of this investigation was to determine transformation frequencies in the presence or absence of heavily damaged cells, using the reliable C3H 10T1/2 assay and a pure β-source described by an exact dosimetry but which is not in direct contact with the cells.

5.3. Materials and Methods

Three sets of irradiation protocols were performed. First, a control set of homogeneous X-ray irradiations, at high dose-rate, and a total dose of 4 Gy: 1a) standard assay, 1b) isolation of cells by frames, 1c) cells growing in agarose trenches. Second, a control set of homogeneous β-irradiations, at low dose-rate, and different doses: 2a) 4.5 Gy, 2b) 13 Gy, 2c) 21 Gy. Third, a set of inhomogeneous β-irradiations at low dose-rate, examining the response of cells in the SF_{65} region (i.e. the dose region with an average surviving fraction of 0.65): 3a) heavily damaged cells were simultaneously present and cells in the SF_{65} region were isolated with frames, 3b) heavily damaged cells were excluded by growing cells in the SF_{65} region in agarose trenches.

5.3.1. Cell culture conditions

C3H 10T1/2 clone 8 mouse embryo fibroblasts, originally established by Reznikoff et al. [18] were obtained from Dr. L. Hieber, Gesellschaft für Strahlenforschung, Munich, Germany, at passage 8. The cells were grown to passage 9 and then frozen in liquid nitrogen. Cells were thawed and grown to give the required number of cells for each experiment. Only cells below passage 15 were used. Stock cultures were grown in 75 cm^2 flasks and never allowed to reach confluence. The cells were maintained in BME medium (Amimed, Muttenz, Switzerland), 10% heat-inactivated fetal bovine serum (Boehringer Mannheim, Germany) and 0.5% gentamycin (Amimed), at 6% CO_2 and 37°C.

24 hours prior to irradiation, cells were plated into Petriperm® dishes (Heraeus, Zurich, Switzerland) with a 25 µm basement foil at a cell density of 2 x 10^4 cm^{-2}. Cells were cultured in two different ways in order to investigate the effects of inhomogeneous radiation fields. Where heavily damaged cells were simultaneously present, cells grew throughout the Petriperm dish (3a). To exclude heavily damaged cells (3b), two molds (2 x 25 x 5 mm) were placed in the Petriperm dish 9 mm either side of the yttrium wire (in the SF$_{65}$ dose region). Growth medium containing 1% agarose (Serva, Walisellen, Switzerland) at 60°C was poured into the dishes and allowed to solidify. The molds were removed and the two resulting trenches washed carefully with PBS (Amimed) to remove any remaining agarose. Cells were then plated only into the trenches (see Fig. 22) at equal cell density = 2 x 10^4 cells cm^{-2}. During the irradiation the cells never reached confluence (microscopically determined).

24 hours prior to the homogeneous ^{90}Y-irradiations 2 x 10^5 cells were plated with 2 ml medium in the central area of a Petriperm dish. After 1.5 hours 3 ml medium was added. This procedure resulted in the cells settling only in the irradiated area at a cell density of about 1.5 x 10^4 cells cm^{-2}, which was necessary because the active ^{90}Y-foil had a dimension of 2.5 x 5 cm, and the cells under these conditions never reached confluence nor grew over the irradiated area (microscopically determined). 24 hours prior to the homogeneous X-ray irradiations cells were plated at a concentration of 2 x 10^4 cm^{-2} throughout the Petriperm dish.

5.3.2. Irradiation conditions

Inhomogeneous β-irradiations were performed using a thin yttrium-90 wire (0,1 x 0,1 x 25 mm) (Johnson Matthey, Cheshire, Great Britain) which had been previously activated with thermal neutrons to an activity of 1.6 x 10^7 Bq per wire. Over 99% of the radioactivity was due to β-decays of ^{90}Y (half-life: 64.1h, mean LET: 180 eV µm^{-1}). The wire was precisely positioned along a midline below the basement growth-foil of the culture dish by means of a Plexiglas disk with a tailored groove (0.2 mm deep). The exposure time lasted 24 hours starting 5.5 hours after neutron activation. The dose across the dish was extremely inhomogeneous. Directly above the wire more than 750 Gy were received during the 24 hours. This rapidly decreased with distance away from the wire. At 20 mm distance the total dose was zero (Fig. 21). Cells were investigated in a region of modest survival (the SF$_{65}$ region), closely adjacent to the heavily damaged cells. The region covered an area between 9 and 11 mm

Figure 21: **Estimated Dose**
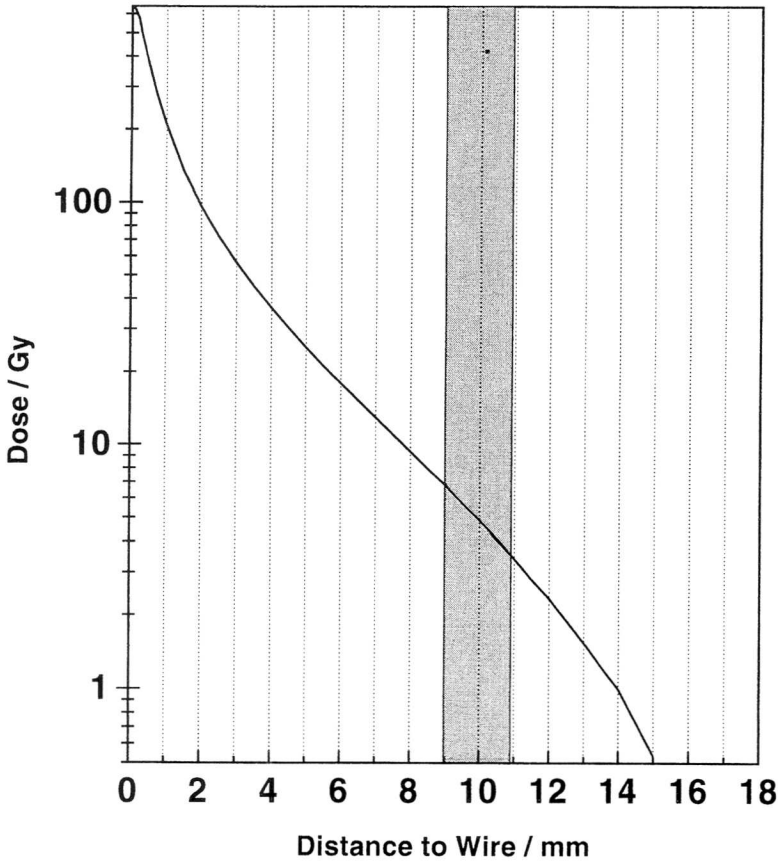
Figure 21: Estimated dose, calculated from Berger point kernel, based on the computer code sadde.2 [38]. Dose was integrated over 24 hours and along the wire and based on integrated activity of yttrium line source: 4.9×10^{11} cm^{-1}. The "distance to wire" is a measure of the distance to a point immediately above the wire along the surface of the basement growth-foil. Shaded area represents the location of the frames and the agarose trenches

Figure 22: Experimental time protocol. Cells were seeded either throughout the dish or into agarose trenches. After 24 hours a radioactive yttrium-wire was attached below the Petriperm foil and fixed exactly at the center by means of a Plexiglas disk. Irradiation lasted 24 hours, and immediately afterwards cells were harvested (either selected by aluminum frames or trypsinized in the agarose trenches) and subjected to the transformation assay. The investigated area was 2 mm wide, 25 mm long, and located 9 mm from the wire.

from the wire (Fig. 22). The total dose integrated over this investigated area and for the 24 hour exposure period was 6 Gy (4 mGy min^{-1}). The variation of the dose over the investigated area was maximally three-fold. Cells closest to the wire received a dose of 9 Gy, and cells furthest from the wire received a dose of 3 Gy. The dose was calculated based on the Berger point kernel. For numerical integration the average β-energy and the scaled absorbed dose distribution from the computer code Sadde.mod 2 [39] were used. The calculations for the specific geometric situation were made according to the Varskin.mod 2 computer code [39]. Backscatter and bremsstrahlung were neglected due to the given geometrical speciation. Since the wire was in a small groove, the decline of dose rate with distance from the wire was quite steep, because at lower angles the electrons must pass through more Plexiglas.

Homogeneous yttrium-irradiations were performed using a neutron activated yttrium foil (2.5 x 5 cm). The exposures lasted 24 hours. Doses were calculated with the Varskin.mod 2 [39] program, backscatter being respected, but bremsstrahlung was neglected. Cells were exposed to the following total doses: 4.5 Gy (3.1 mGy min^{-1}), starting activity of the foil was 1.0 x 10^5 Bq cm^{-2}; 13 Gy (9 mGy min^{-1}), starting activity of the foil was 3.1 x 10^5 Bq cm^{-2}; or 21 Gy (14.6 mGy min^{-1}), starting activity of the foil was 5.1 x 10^5 Bq cm^{-2}. Homogenous, high dose-rate X-ray irradiations were also performed (4 Gy X-rays, 240 keV, 6.3 mA, 0.9 Gy min^{-1}).

The time protocol of the inhomogeneous-irradiation experiment is schematically presented in Figure 22. For each treatment, 8 Petriperm® dishes were irradiated and 4 Petriperm® dishes were sham-irradiated. Immediately after exposures in the presence of heavily damaged cells, cells to be measured were isolated from the SF$_{65}$ dose region by removing the medium, washing with PBS-CMF (Amimed), and placing aluminum frames of rectangular shape (25 x 2 mm inner width) at precise positions using a mask inserted under the transparent growth foil. The frames were fixed *in situ* using silicone grease which simultaneously functioned as a seal. They were filled with Trypsin-EDTA (Amimed) to remove the cells. Trypsinization was stopped with medium containing serum. Cells were counted and plated into 9 cm dishes at a concentration of 3000 cells per dish for the transformation assay and 700 cells per dish for the colony-forming ability assay. Sham-irradiated cells isolated in an identical manner were diluted to a concentration of 1500 cells per transformation dish and 500 cells per survival dish. These cell concentrations yielded 1.5 to 4 viable cells per cm^2 for the transformation assay. Immediately after exposures, in the absence of heavily damaged cells, cells in the agarose

trenches were washed with PBS-CMF, trypsinized and diluted to the same concentrations as described above. High dose-rate X-ray controls were also conducted with identical protocols except for the shorter exposure times. Immediately after both sets of homogeneous irradiations, cells were trypsinized and diluted to 100 surviving cells per dish to quantify survival and 200 surviving cells per dish to quantify transformation according to the standard assay. These cell concentrations also yielded 1.5 to 4 viable cells per cm^2 for the transformation assay.

Transformation dishes were incubated for six weeks with weekly renewal of medium. Confluency was reached after about 14 days. Cells were washed with PBS-CMF, fixed with methanol and stained with Giemsa (10%, Merck, Zurich, Switzerland). Survival dishes were fixed after 9 days. Colonies with more than 64 cells were scored as survivors. Cell transformation was assessed using the morphologic criteria described by Reznikoff [18]. Only type II and type III foci were scored as transformants. Transformation frequencies per survivor were calculated according to the criteria described by Han and Elkind [36] and assume the transformed clones appear in the petri dishes with Poisson probabilities. Transformation frequencies were derived from pooled results of all experiments. Standard errors are calculated according to the method of Balcer-Kubicek et al. [37] SE $= \pm \sqrt{\frac{1}{n} - \frac{1}{M}}$, where n is the number of dishes without foci and M is the number of total dishes.

5.4. Results

Percent survival after inhomogeneous yttrium-irradiation in the investigated area was 66.1 ± 2.83 in the presence of heavily damaged cells and 62.2 ± 12.3 in the absence of heavily damaged cells. These values are not significantly different (Table 1). Plating efficiencies lay between 10 and 30%, which is somewhat lower than we routinely observe with C3H 10T1/2 cells in our laboratory (between 30 and 40%) and is attributed to the additional handling and/or growth in Petriperm dishes.

During the 24 h inhomogeneous exposures, the integrated dose fell sharply across the radiation field from approximately 750 Gy directly above the wire to zero Gy at the edge of the dish (Fig. 21). Proximal to the yttrium wire, the high doses caused both cytotoxicity and cellular detachment. The transformation frequency per viable cell was 10.6 x 10^{-4} for cells exposed in the presence of heavily damaged cells and was 1 x 10^{-4} for cells in the absence of heavily

TABLE 1:

Surviving fractions and transformation frequencies after various radiation setups to investigate the effect of inhomogeneous β-irradiation

Number in rectangular brackets gives number of independent experimens.

a: Survival rate

b: Standard error

c: Number of total dishes

d: Number of dishes without foci

e: Number of viable cells per transformation dish

f: Average number of foci per dish = $-\ln\left(D/M\right)$ [36]

g: Transformants per surviving cell with standard error (SE) = $\pm\sqrt{1/n - 1/M}$ [37]

h: One extreme outlier was rejected (whole control experiment).

Nr.	Treatment	SF^a	se^b	M^c	n^d	S/D^e	λ^f	$f^g \times 10^{-4} \pm 1\ SE$
1a	Control X-ray, 4 Gy, standard assay	24.5	1.97	48	37	180	0.26	14.5 ± 4.37
1b	Control X-ray, 4Gy, selection by frames	21.8	3.00	50	40	146	0.22	15.3 ± 4.84
1c	Control X-ray, 4Gy, agarose trenches	22.8	1.73	43	33	175	0.26	15.1 ± 4.80
	Sham-irradiation, standard assay [14]	100	8.92	373	368	218	0.01	0.6 ± 0.29
	Sham-irradiation, selection by frames [3]^h	100	7.50	94	94	209	0.00	0.0 ± 0.00
	Sham-irradiation, agarose trenches [5]	100	16.71	102	100	227	0.02	0.8 ± 0.55
2a	Homogeneous Y-irradiation, 24 h, 4.5 Gy [3]	52.4	4.56	150	136	227	0.09	4.3 ± 1.15
2b	Homogeneous Y-irradiation, 24 h, 13 Gy [5]	21.7	1.56	248	228	89	0.10	9.4 ± 2.10
2c	Homogeneous Y-irradiation, 24 h, 21 Gy [3]	11.9	0.45	114	91	129	0.22	17.0 ± 3.70
3a	Background of heavily damaged cells, Yttrium, 6 Gy, 24 h, [4] (selection by frames)	66.1	2.83	185	151	193	0.20	10.6 ± 0.18
3b	Without background of heavily damaged cells, Yttrium, 6 Gy, 24 h, [5] (agarose trenches)	62.2	12.33	207	199	382	0.04	1.03 ± 0.35

damaged cells (Table 1), a ten-fold difference. These transformation frequencies and standard errors are pooled results of all independent experiments and are based on the method of Han and Elkind [36]. The experimental means and interexperimental errors are 1.22 x 10^{-3} ± 0.27 x 10^{-3} transformants per survivor for cells exposed in the presence of heavily damaged cells (3a) and 0.13 x 10^{-3} ± 0.054 x 10^{-3} for cells exposed in the absence of heavily damaged cells (3b). A *t*-test analysis of these values indicates, they are significantly different at the 0.01 level. The dose in the investigated SF_{65} region varied no more than three-fold across the 2 mm trench. To exclude the possibility of artefacts caused by the experimental set-up, control experiments were conducted with 4 Gy high dose-rate (0.9 Gy min^{-1}), X-ray exposures. The resulting frequencies were 15.1 x 10^{-4} and 15.3 x 10^{-4}, for cells selected with aluminum frames and for cells in the agarose trenches, respectively. Cells were also exposed to a homogeneous field of low dose-rate ^{90}Y-irradiation and examined for transformation. The exposures also lasted 24 hours. 4.5 Gy resulted in a transformation rate of 4.3 x 10^{-4}; 13 Gy gave 9.4 x 10^{-4}; and 21 Gy gave 17 x 10^{-4} transformants per survivor (Table 1).

5.5. *Discussion*

We have developed an *in vitro* model-system employing a thin, β-emitting yttrium-90 wire, to produce extremely inhomogeneous radiation fields in order to investigate hot particle effects on induction of cellular transformation. C3H 10T1/2 cells within the SF_{65} dose region of the inhomogeneous irradiation field were isolated following exposure and examined by a standard transformation assay. Either heavily damaged cells were simultaneously present during exposure or they were excluded by localising cells to the SF_{65} dose region by means of an agarose trench. The frequency of transformation observed in cells exposed to a background of heavily damaged cells was enhanced ten-fold at equivalent cytotoxicity.

The investigated dose region was chosen because the surviving fraction of 0.65 results in reasonably high transformation rates. The SF_{65} dose region under both conditions was identical with respect to dose, dose-rate and cell density. The high dose-rate X-ray control experiments demonstrate that neither the agarose nor the method of isolating cells by means of aluminum frames had a measurable bias on the transformation frequency under high dose-rate conditions. The transformation values are routinely obtained in our laboratory and have been reported in the literature [36].

Following the 24 h exposure to ^{90}Y, cells from both inhomogeneous irradiation field set-ups were treated in exactly the same manner. The only obvious difference between the two set-ups was that in one case intercellular signalling from heavily damaged cells was possible, either via cell-cell contact or via the medium, but in the other case, heavily damaged cells were not present. It seems unlikely, but we cannot exclude the possibility that differences in the yields of radiation breakdown products in the media contributed to the enhanced transformation frequency (64). The transformation frequencies after 4.5 Gy and 13 Gy low dose-rate β-irradiations were comparable to the transformation frequencies obtained by Han *et al.* after low dose rate γ-irradiations (5 mGy min^{-1}). 4.5 Gy β-irradiation (3.1 mGy min^{-1}) resulted in 4.3 x 10^{-4} transformants per survivor, 4.5 Gy γ-irradiation in 5 x 10^{-4} transformants per survivor (Han *et al.* [65]); 13 Gy β-irradiation (9 mGy min^{-1}) resulted in 9.4 x 10^{-4} transformants per survivor, 13 Gy γ-irradiations in 7 x 10^{-4} transformants per survivor (Han *et al.* [65]). In our experiments, the transformation frequency after 4.5 Gy low dose-rate β-irradiation was three-fold lower than after high dose-rate X-ray irradiation. 13 Gy homogeneous β-irradiation induced approximately the same transformation frequency as 6 Gy from the inhomogeneous set-up in a background of heavily damaged cells which corresponds to a two-fold enhancement with respect to total dose.

Transformation has been demonstrated to be a multi-step process. As the difference observed here was caused during the 24 h of exposure, it probably relates to the initiating event caused by radiation damage. The difference appears to be associated with the heavily damaged, highly irradiated cells. Some form of signal either passively or actively induces a state of enhanced transformation-frequency in non-lethally irradiated cells. We have not yet succeeded in isolating the signalling agent.

Terzaghi and Little [66] described that enhanced transformation results from potentially lethal damage repair, and Kennedy and Little [33] demonstrated that a state of enhanced transformation is induced in cells by ionizing radiation. We examined foci and clones from colonies of radiation-induced C3H 10T1/2 transformed cells and observed a state of genetic instability causing multiple polyploidy events [67]. Although the molecular basis for these responses associated with enhanced transformation frequencies is not known, its induction is not necessarily a direct effect of radiation. In studies of low-dose α-particle exposures, sister chromatid exchanges [60,61] and p53 expression [62] were observed in an unexpectedly high proportion of cells. In these studies a bystander effect was indicated on microsimetric grounds because more cells

than those whose nuclei were physically traversed by an α-particle displayed the induced response. It has been demonstrated that on average more than one α-particle is required to inactivate C3H 10T1/2 cells [68]. Therefore, the bystander effect does not necessarily depend of cell inactivation.

Various explanations for possible signals between differently damaged cells can be found in the literature. Expression of DNA damage-induced (DDI) genes is expected to be high in heavily damaged cells promoting enhanced release of a spectrum of damage-associated cytokines including TGFβ and TNFα. Important DDI genes that are induced by radiation are the protooncogenes c-fos, c-jun, jun-B and c-myc. They all code for nuclear transcription factors and have been discussed as critical target genes in radiation carcinogenesis [69]. TGFβ and c-myc have been found overexpressed in morphologically transformed C3H 10T1/2 cells [70], and transfection of untransformed cells with c-myc resulted in increased transformation [71]. Another interesting DDI gene is basic fibroblast growth factor (bFGF). It serves as an enhancer of potentially lethal damage repair via an extracellular autocrine loop and enhances DNA synthesis in untransformed C3H 10T1/2 cells [72]. Dead and dying cells also release DNA fragments [73] which have demonstrable transformation activity. The factor of ten difference we observed is about as high as is observed after extreme protraction of γ-ray dose to 0.1 Gy/day (0.07 mGy min^{-1}) [36]. It is also as high as promoter-enhanced transformation, e.g. TPA [74].

The transformation enhancing effect observed in this *in vitro* system may also apply to *in vivo* situations, *e.g.* hot particle effects after deposition in the lung. The risk of inhaled hot particles has been discussed for more than 20 years (for review see [8, 14] and theoretical modelling suggests the primary risk is carcinogenesis. However, few *in vitro* experiments have been done to verify this theoretical data. In the studies described here β-emitting hot particles were used to produce an extremely inhomogeneous β-radiation field. Cells in close proximity to the β-radiation source were heavily damaged because of ultra high dose-rates and high cumulative doses and resulted in microlesions. Cells adjacent to these microlesions not only received lower doses but also a spectrum of associated cell trauma signals and had an enhanced risk of transformation. Our results suggest that the inhomogeneous radiation fields produced *in vivo* around hot particles cause an elevated risk compared to equivalent doses from homogeneous fields.

6. GENOME LABILITY IN RADIATION-INDUCED TRANS-
FORMANTS OF C3H 10T1/2 MOUSE FIBROBLASTS

Nigel E. A. Crompton, Martina Sigg, Rolf Jaussi.

6.1. ABSTRACT

We have been investigating radiation-induced transformants of C3H 10T1/2 mouse fibroblasts for evidence of heritable changes. C3H 10T1/2 cells were treated with 8 Gy X-rays. After approximately eight weeks culture, type II / III foci were isolated from the monolayer using cloning rings. Cell lines developed from these foci, and clones established from these cell lines, were examined for DNA content. The isolated focal lines and derived clones often display aneuploidy and/or polyploidization. In one instance a clone (derived from a single cell) displayed multiple polyploidies. During passage the ploidy of many of the anomalous populations gradually reverted to the ploidy of the non-transformed state. The morphological features associated with the transformation event were, nevertheless, retained. The results demonstrate that exposure to radiation can induce, in association with morphological transformation; a heritable, genomically labile state.

6.2. INTRODUCTION

The quadratic form of the mutation induction curve observed after very low dose-rate continuous irradiation of V79 Chinese hamster lung fibroblasts [75] indicates a multi-hit (probably two-hit) phenomenon is involved. Based on expected double-strand break frequencies, a model can be developed where two double-strand breaks in a target the size of a replicon loop result in deletion mutation events. However, the protracted exposure periods require the first such break to be stably inherited over many cell generations until the second break occurs and the deletion is generated. An alternative model, similar to that proposed by Kennedy et al. [76], assumes some form of heritable premutational change is induced; either a lesion associated with the chromatin, or a new pattern of gene expression. A second event in this premutational background then leads to the mutation. At higher dose levels, induced repair processes would be associated with mitigation of this premutational change. Kennedy and

her colleagues demonstrated that following a 4 Gy dose of X-rays, transformation frequency was independent of the number of cells irradiated. They concluded that some change was induced by the radiation exposure which was transmitted to the progeny of the surviving cells and resulted in an enhanced frequency of morphological transformation [33]. We report here that the radiation-induced transformation phenotype is frequently associated with genomic lability and in particular with a tendency to undergo polyploidization.

6.3. MATERIALS AND METHODS

6.3.1. Cell culture

The C3H 10T1/2 clone 8 mouse embryo fibroblasts were obtained from Dr. L. Hieber, Gesellschaft fuer Strahlenforschung, Munich, Germany. The cells were exposed to radiation in order to induce morphological transformation at passage 13. All cells were maintained in BME medium (Amimed), 10% heat inactivated fetal bovine serum (Boehringer Mannheim), 0.5% gentamycin (Amimed), at 6% CO_2, 37°C.

Isolation of morphological transformants and their clones. Cells of passage 13, which have never been allowed to grow to confluence, were plated in 75 cm^2 culture flasks. 24 h after plating they were exposed to 8 Gy X-rays at 0.9 Gy min^{-1}. Immediately after irradiation the cells were washed with PBS, harvested and plated in 9 cm dishes at a cell concentration of 2-3 survivors per cm^2. Cells were maintained in culture for more than eight weeks with weekly renewal of the medium. After 58 and 66 days foci were isolated from a total of eight dishes. Foci were scored according to the criteria of Reznikoff et al. [18]. They were isolated by trypsinization in a small isolation ring placed around the colony. The isolated focal lines were allowed to grow and from them cell clones were developed. Cells were harvested and then inoculated into 24 multiwell plates, at a concentration of one cell per well. The 24 multiwell plates were regularly monitored until colonies had grown. Cell clones were taken from those wells where only a single colony had been observed during the whole growth period. Any indication of satellites or non-circularity excluded a colony for isolation.

6.3.2. Flow cytometry

Age distribution curves were measured using a Becton Dickinson FACScan flow cytometer and cell cycle phase fractions analyzed by MCYCLE analysis (Phoenix flow systems). Cells were prepared for flow cytometry according to standard procedures [77]. Briefly, the cells were harvested; cells in monolayer required handling with trypsin and a PBS wash. Cells were fixed in 70% alcohol for at least 4 h. The cells were centrifuged (300 x g), the fixative discarded and 500 ml pepsin (2.5 mg ml^{-1}) was added for 5 min, 2 ml PI (propidium iodide) was added (2 mg ml^{-1}) for 1 min, and finally 120 ml of RNase was added (45 mg ml^{-1}) for 5 min.

6.4. RESULTS

6.4.2. Isolation of lines

Two sets of radiation-induced morphological transformants were isolated with a period of approximately one year separating the two experiments. Foci were chosen based on their highly transformed type II / III appearance [18]. All of the focal lines had individual characteristic morphologies. During the first experiment six focal lines were isolated (5, 6, 7, 9, 11, and 13). From these lines clones were established. Four clones were established from the focal line 11 and from one of these a further round of cloning resulted in the establishment of 14 more lines. During the second experiment thirteen foci were isolated, only four of these lines (1, 3, 7, and 8) were used to establish clones. In both experiments a total of 19 foci were isolated from which a total of 63 clones were established.

6.4.2. Genome lability

The DNA content of the radiation-induced morphologically transformed lines was examined. Both focal lines and clones of these lines were investigated. A control line was derived from a patch of irradiated but non-transformed monolayer of C3H 10T1/2 cells surrounding radiation-transformed foci. Although the cells originate from mice which have a diploid chromosome count of 40, our parental C3H 10T1/2 cells have an average of 68 chromosomes reflecting a hypotetraploid state. The control line had the same DNA content as the "normal" parental hypotetraploid line. Line 13 and 9 had a DNA content

86% that of the parent. Line 11 displayed multiple G1 peaks. It also had a G1 peak with 86% that of the parent. However, the major G1 peak had the parental DNA content. A third, minor G1 peak had 71% that of the parental DNA. Its corresponding G2 peak was also visible and these peaks may reflect hypotriploidy subpopulation.

Cells from line 11 were cloned to determine which of the multiple G1 peaks was associated with the morphological transformation. Four clones were established. Two of the clones displayed the hypotetraploid condition, however, in both cases the presence of an extensive G2 peak may indicate additional hypooctaploid cells. The third clone displayed an additional minor hypohexaploid cell population. The fourth clone was highly anomalous displaying not only a minor hypotetraploid peak but also major hypohexaploid and hypooctaploid peaks. Although differences in the general morphology of the cells between lines was observed, none of the lines reverted to the parental state. The morphological features associated with the transformation event were retained in all the cloned lines.

In order to establish if single cells were producing populations of cells with multiple ploidies this fourth highly anomalous population was subjected to a further round of cloning. Extensive precautions on a day by day basis were taken to ensure that only those colonies growing from single isolated cells were selected. Any question as to the fulfilment of this requirement meant automatic rejection of the colony. Fourteen such colonies were isolated. Representative DNA content distributions are presented in figure 23. Six of the fourteen clones displayed the parental hypotetraploidy at the time of measurement (A). Two clones displayed stable hypooctaploidy up to passage 8 (B) and 9. The other 6 clones demonstrated unstable multiple ploidies. Panels C-D and E-F display hypooctaploid populations which during the course of four and three passages, respectively, developed major populations of hypotetraploid cells. Panels G-H demonstrate a similar transition but from a hypododecaploid population to a hypotetraploid population. Chromosome preparations of the hypododecaploid population revealed about 200 chromosomes per cell. The DNA content of the most anomalous clone is presented in figure 24. Here multiple ploidies were observed including: hypotetraploid, hypohexaploid, hypooctaploid, hypodecaploid and hypododecaploid. With time in passage the population became hypooctaploid. Chromosome preparations of this clone revealed about 120 and 150 chromosomes per cell by passage 5 (Fig. 24B) and about 120 chromosomes per cell by passage 7 (Fig. 24D).

68

Figure 23: DNA Histograms
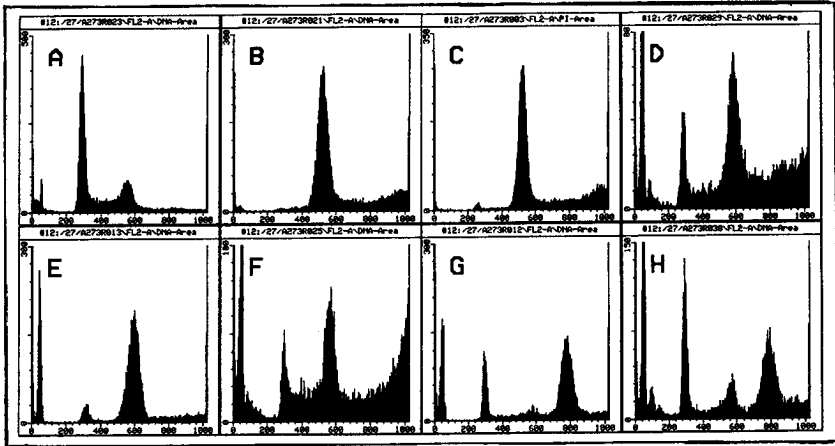
Figure 23: Histograms of DNA content of lines established from a second course of cloning of the clone 11. A: a hypotetraploid clone at passage 7, B: a hypooctaploid clone at passage 8, C-D: shift of a hypooctaploid to a hypotetraploid clone during passage 5 to passage 9, E-F: shift of a hypooctaploid to a hypotetraploid clone during passage 6 to passage 9, G-H: shift of a hypododecaploid to a hypotetraploid clone during passage 5 to passage 8. The hypooctaploid and hypododecaploid G1 peaks have been adjusted to approximately the same heights, in panels C+D, E+F and G+H, to emphasize the increasing proportion of hypotetraploid cells observed with time in culture.

Figure 24: DNA Histograms
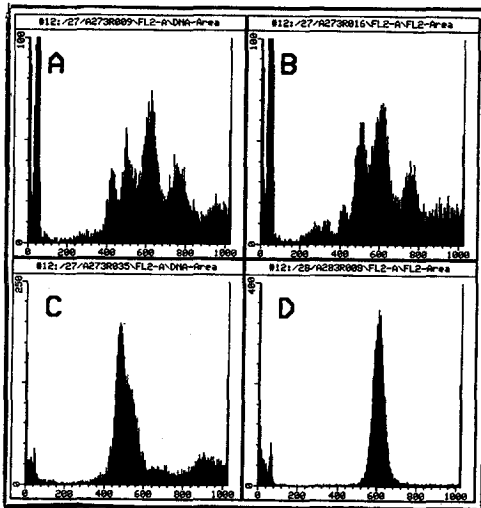
Figure 24: Histograms of DNA content of the "D-6A" clone. The clone displays multiple polyploid states which shift to a single hypooctaploid state during passage in culture. A: passage 4, B: passage 5, C: passage 7, D: passage 9.

Figure 25: DNA Histograms
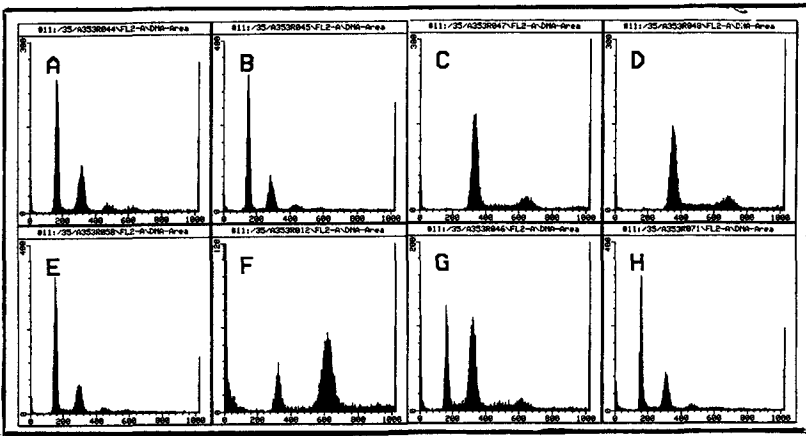
Figure 25: Histograms of DNA content of cells and clones derived from a radiation-induced morphologically transformed focus. A: passage 8 of the focal line, B: clone "a5" passage 3, C: clone "b3" passage 2, D: clone "c5" passage 3, E: passage 10 of the focal line, F-H: shift of the ploidy of clone "a6" to the ploidy of the original focal line during passage in culture, F: passage 2, G: passage 5, H: passage 6.

in the first study six focal lines were examined for anomalous ploidy. At the time of measurement three lines displayed the parental DNA content and three were anomalous. In the second study thirteen foci were studied. At the time of measurement seven focal lines displayed the parental DNA content and six were anomalous. Figure 25 displays the DNA content of one of these lines and four clones isolated from it. Two of the clones are hypooctaploid (C-D). The focal line (A) and one of the clones (B) are hypotetraploid, however, they both display an extensive "G2" peak which indicates hypooctaploid cells are also present. This is supported by the population dynamics data of the fourth clone (panels F-H). During passage the major hypooctaploid peak (panel F) is gradually replaced by a hypotetraploid peak (panel G) until the ploidy distribution attains that of the original focal line (panel H), which was stable during passage (A+E), and its comparable clone (B).

6.5. DISCUSSION

Morphological transformation of the C3H 10T1/2 mouse fibroblast cell line is frequently observed in association with a number of other phenotypic characteristics often considered surrogate markers of tumorigenicity. Such properties include amongst others ability to grow at elevated cell densities, ability to grow in semi-solid media (anchorage independence), ability to grow in media with low levels, or in the absence, of serum. Here we describe a further phenotype associated with radiation-induced transformation; polyploidization. DNA content has been examined previously in spontaneously arising and chemically-induced morphological transformants [78]. These studies produced little evidence for polyploidization. 80% of the clones had lost significant amounts of DNA from their genomes during the five to six passages required for their establishment. Just two of the 75 clones displayed an increase in DNA content. Both cases may be examples of hypohexaploidy. The two lines were tumorigenic in nude mice and had been induced by exposure to methyl nitro-nitrosoguanidine.

In the present study polyploidization was observed to occur at high frequency in the radiation-induced transformed foci. It was not observed in cells from the monolayer surrounding the foci. About 50% of the transformed focal lines were found to display the phenomenon, although the true frequency may be higher because many of the populations lose their high ploidy states with passage in culture. 22 of the 32 clones, derived from such focal lines, displayed polyploidization. Most of these clonal populations displayed multiple polyploidy

even though they were derived from single cells. Clearly, the genomes of these cells are labile. Hypoaneuploidy was observed in some of the morphologically transformed lines, as has been previously reported for C3H 10T1/2 transformants [78]; but most striking were the shifts in ploidy which ranged from hypotriploidy to hypododecaploidy.

Great care was taken to ensure the lines arose from single cells during the cloning procedures. We, therefore, assume that essentially all the clones had a single cell origin and that the multiple ploidy populations observed were descendents of single cells. The chromosome counts confirmed that the high DNA contents were due to multiple sets of chromosomes. Hypooctaploidy could result from an aberrant anaphase, however, this hypothesis is not sufficient to explain the four hypohexaploids, a hypodecaploid and two hypododecaploids (nor the small number of hypotriploids) observed. We plan to examine the centrosome for multiple centrioles. Radiation-induced morphological transformation in Balb/3T3 cells has been reported to be associated with the presence of viral C-type particles [79]. Virus-like particles are found localized to centrioles in both Chinese hamster and mice cells [80, 81, 82].

The polyploid populations were usually unstable and in many cases reverted to the hypotetraploid state with time in culture. There were exceptions. Some of the populations were stably hypooctaploid for the duration of observation and in one instance a multipolyploid population did not revert to the hypotetraploid state but became hypooctaploid. In at least one case a stable ratio of hypotetraploid to hypooctaploid was observed in the focal line and two of its clones. As no significant polyploidy has been reported for spontaneously arising or chemically-induced morphological transformants [78], it appears to be a consequence of the action of the radiation. Kennedy et al. have demonstrated that radiation induces a persistent change in C3H 10T1/2 cells which causes a greatly increased frequency of morphological transformation [33]. This phenotype is associated with a number of other characteristics (examples include anchorage independence and growth at high cell density) at frequencies higher than expected if these characteristics were caused by independent gene mutations. Another characteristic reported here, with a frequency of almost 50%, is polyploidization. In order to accommodate these findings it has been suggested that epigenetic mechanisms may result in quantitative changes in the expression of a number of genes rather than their mutation [78]. Radiation-induced priming of labile genetic elements or retroviruses could be the basis of such an epigenetic mechanism. Alteration of

methylation patterns has been suggested as a cause of persistent hypersensitivity to mutation induced by X-ray exposure [83].

We have demonstrated that the radiation-induced transformation phenotype is frequently associated with genomic lability and in particular with a tendency to undergo polyploidization. However, the distribution of polyploidy within clonal populations displaying this phenomenon is not fixed. There is often a reduction in higher ploidy levels associated with subsequent cell growth and passage. This usually resulted in reversion of the population to the hypertetraploid parental state but also resulted in populations displaying stable but anomalous polyploid states.

7. DISCUSSION

A cell culture model has been developed to assess stochastic and non-stochastic β-hot-particle effects *in vitro*. As end-points cell survival and transformation were quantified.

Yttrium-90 was chosen as the radiation source because of its pure, high energy electron radiation, the easy of handling of the foil and small wires, and the reasonably high neutron cross-section of its precursor. The short half-life of 64 h did not permit irradiations at a constant dose rate. At the end of a 24 hour experiment dose rate was 76% of the initial rate. Directly above the wire, the integrated deposited dose was more than 900 Gy. This rapidly decreased within a few cell diameters to zero Gy at 20 mm distance. This inhomogenity is mirrored in the cytotoxicity observed in the irradiated cells. Directly above the wire-source, cell loss and necrosis could be observed, whereas cell survival was essentially 100 % at distances of more than 12 mm from the wire-source, where the dose was practically zero.

In the colony forming assay a strong dose-rate effect was observed. At 40 Gy total dose (30 mGy min^{-1}) the surviving fraction was 0.01, at 20 Gy (14 mGy min^{-1}) 0.2, at 10 Gy (7 mGy min^{-1}) 0.65 and at 5 Gy (3.5 mGy min^{-1}) 0.9. These values of colony-forming ability are in the range of other low dose-rate γ-ray experiments reported in the literature [54]. That implies, that the revised dosimetry predicts reasonable survival values.

Varskin Mod2 is a widely used and widely approved semi-empirical code, assessing the radiobiological risks resulting from radionuclide contaminations of tissues [84]. Its use for this cell culture system is reasonable, because all parameters could be determined and estimated. The only uncertainty comes from the backscatter correction. The Berger point kernel is based on measurements where the radiation source was surrounded by an infinite water medium. For very thin sources that are bounded on one side by air, no backscatter occurs. Self-shielding of the source was also neglected, since this only plays a role with low-energy β-emitters [59].

The radiation-induced transformation rate of C3H 10T1/2 cells was 10-fold higher in an *in vitro* system, when simultaneously heavily and non-lethally damaged cells were present, than in a situation with identical exposure rates, but where heavily damaged cells were excluded.

The investigated dose region in both systems was identical with respect to dose and dose rate. Care was also taken to ensure exposures were performed at identical cell densities. Neither the agarose nor the way of isolating cells by

means of aluminum frames had an influence on the transformation rate as demonstrated in the control X-ray experiments. With 4 Gy X-ray a transformation rate of 1.4×10^{-3} transformants per survivor was obtained which corresponds to values reported in the literature [85, 36]. The investigated dose region between 9 and 11 mm distance from the wire-source is in itself inhomogeneous, the total dose varying between 2.5 and 9 Gy (fig. 26). However, this variation is identical for both set-ups. After the 24 h Y-90 exposure, the cells of both systems were immediately treated in exactly the same manner. The different transformation rate is, therefore, attributed to the different conditions during exposure.

Various factors can be postulated to have played a role. Since both experimental set-ups differ only in the first 24 hours, during the exposure have to occur either a different amount of initiated damage or different damage fixation and repair.

The fact that highly damaged or even dying cells are able to influence the transformation rate has been previously described by van Bekkum and Bentvelzen [73]. They showed that mechanically destroyed cells, or even DNA alone, in the medium of an *in vitro* system enhanced transformation frequency [86,87]. Especially at doses above 100 Gy, enough DNA breaks were induced in so-called donor cells to produce fragments that directly enhanced transformation in recipient cells. They found a linear relationship between DNA concentration in the medium and the frequency of transformation. Under the *in vitro* conditions it was calculated that on average 1 pg of DNA has to be available per cell to yield one transformant per 3×10^5 exposed cells. However, under *in vivo* conditions, extracellular DNA fragments are subjected to destruction by extracellular DNA nucleases, which cause a rapid degradation of the DNA with time. In our inhomogeneous radiation fields interphase death occurred in the most severely damaged cells, causing potential release of many DNA fragments into the medium.

The bystander effect describes a phenomenon where non-exposed cells in the vicinity of damaged cells exhibit damage. In human lung fibroblasts and in CHO cells which were irradiated with very low α-doses, significantly more cells displayed sister chromatid exchanges than whose nuclei where traversed by an ionizing particle [60, 62]. The mechanism of induction of the bystander effect remains to be elucidated. Our system does not represent strictly a bystander situation, because the investigated cells were exposed to sublethal doses of ionizing radiation.

Figure 26: Dose Variance along the Wire
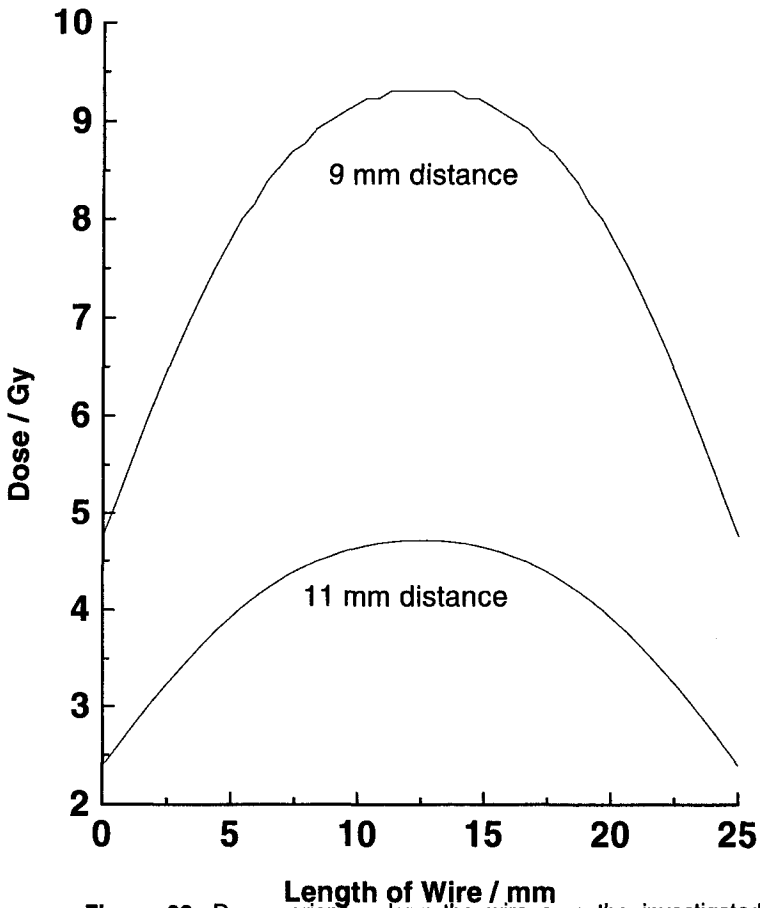
Figure 26: Dose variance along the wire over the investigated area. The integrated dose over the area between 9 and 11 mm distance from the wire was 6 Gy. Calculating the dose for various targetpoints along the length of the wire results in dose curves. The upper represents the dose curve at 9 mm distance to wire, the lower represents the dose curve at 11 mm distance to wire. The "distance to wire" is a measure of the distance to a point immediately above the wire along the surface of the basement growth-foil.

DNA-damage-induced genes (DDI genes) may play an important role as transducers of signals and as mediators of cancer initiation and development (for review see [88]). The 1994 UNSCEAR report [89] lists some 40 growth arrest and DNA-damage-inducible genes that are stimulated by doses of a few milligray to a few gray of ionizing radiation. They induce replication at an inappropriate time with respect to the normal cell cycle. Either overreplication or induction of certain genes have long-term consequences which may alter the cellular phenotype and the genetic constitution of cells.

Terzaghi found in her studies of irradiated rat tracheal epithelial cells two types of cell interaction [90]. One type appeared to involve direct cell-cell contact as occurs within intact tissues. The other type appeared to be mediated via a diffusible factor, most likely TGFβ which exerted a selective effect against the growth of normal cells but permitted initiated cells to survive and proliferate. In mouse skin exposed to Sr-90 (between 1 and 50 Gy), $TGF\beta_1$ mRNA expression was increased 200% above controls [91]. Direct cell-cell contact in the vicinity of a hot particle occurs *in vivo* as well as in our *in vitro* system. The influence of diffusible factors *in vivo* will certainly be dependent on extracellular conditions which will effect whether the factor is stable, transported to and resorbed by other cells.

Important DDI genes that are induced by radiation are the protooncogenes c-*fos*, c-*jun*, *jun*-B and c-*myc*. They all code for nuclear transcription factors and have been discussed as critical target genes in radiation carcinogenesis [92, 69]. C-*myc* has been found to be elevated in X-ray transformed C3H 10T1/2 cells [93], and transfection of untransformed cells resulted in enhanced transformation [71]. However, direct involvement in the transformation process might only occur in later stages of promotion and progression. Leuthauser *et al.* [94] found that the enhanced levels of *myc* mRNA observed in transformed 10T1/2 cells was a result of a process that occurred after the cell had been initially transformed. In human leukemia cells and skin fibroblasts enhanced expression of c-*jun* protooncogene was time, dose and dose-rate dependent [95]. Decreasing the dose rate from 14.3 Gy/min to 0.67 Gy/min was associated with increases of c-*jun* transcripts, and in human lymphoblastoid cells mRNA expression of c-*fos*, c-*jun*, c-*myc* and c-Ha-*ras* was highest at 0.5 Gy [96]. These are indicators that transformation enhancing signals might come from the cells outside the investigated area receiving a lower dose.

Another interesting DDI gene is basic fibroblast growth factor (bFGF). It was found to be X-ray inducible in aortic endothelial cells [97]. It serves as a potent inducer of potentially lethal damage repair via an extracellular autocrine loop

and enhances DNA synthesis in untransformed 10T1/2 cells [72]. Krämer *et al.* [98] have found in UV irradiated HeLa cells that bFGF and interleukin-1 were released into the culture medium. When given to unirradiated cells, these induced the transcription of several UV-inducible genes. They found two possible mechanisms of secretion into the medium; one from the intact cells and one from lysed cells. bFGF and interleukin-1α are active components of so called "extra-cellular protein synthesis-induced factors" (EPIF). EPIF was suggested to cause a 2.8-fold enhancement of the mutation rate in non-irradiated mouse T-lymphoma cells when they were exposed to conditioned medium from UV-irradiated cells [99].

Members of the protein kinase C gene family have been shown to play an important role in tumor promotion and regulation of cell growth. Increased expression of PKC in the absence of other cellular changes was sufficient to cause a loss of cell growth control. The induction of PKC by low-LET radiation was dose and dose-rate dependent in SHE fibroblasts [100]. The induction of PKC mRNA occurred at a time when total cellular transcription was reduced following radiation at doses as low as 0.1 Gy. Down-regulation of PKC by phorbol ester totally blocked the response to X-rays [101]. The induction of transcription factors *jun* and *egr*-1 in X-irradiated human epithelial cells was mediated by a PKC-dependent pathway [102]. The mRNA levels increased in a time- and dose-dependent manner. EGR1 and JUN were rapidly and transiently expressed in the absence of *de novo* protein synthesis after ionizing radiation exposure. They may regulate the late response genes PDGF and TNF-α. However, C3H 10T1/2 cells that stably overproduced PKC displayed neither a transformed morphology nor growth in soft-agar [103].

Cellular transformation can result from incomplete DNA-repair. Terzaghi [66] showed that incomplete repair of radiation damage enhanced the transformation frequency of C3H 10T1/2 cells. DNA lesions are repaired by a two phase mechanism [104]. The first phase is quick and increases cellular survival but is error-prone, the second is slower and completes repair of double strand breaks but is almost error-free. A possible explanation for the enhanced transformation rate observed in inhomogeneous radiation fields is enhanced incomplete repair. The repair processes are disturbed, *e.g.* by cell cycle disturbances or cell proliferation, at an inappropriate time and repair processes are interrupted [105]. Following ionizing radiation cell cycle delays occur, during which DNA-repair is performed. This was shown to be dose-rate dependent [106]. HeLa and V79 cells exhibited a threshold for mitotic delay at 0.1 Gy/hour and at higher dose-rates a linear relationship between dose-rate and mitotic

delay. The average dose-rate in the SF_{65} dose region was 0.25 Gy/hour, which induced little mitotic delay permitting little DNA repair. TGFβ, EGF and PDGF are able to release growth arrested C3H 10T1/2 cells [107].

An enhancement by a factor of 10 is about as high as found by extreme protracting of γ-ray dose to 0.1 Gy/day (0.07 Gy min $^{-1}$) [36]. It is in the region of promoter enhanced transformation, e.g. by TPA [74]. TPA activates the PKC pathway, increasing the diacylglycerol concentration, and results in an enhanced transformation rate.

Low dose-rate 60 Co γ-ray experiments with C3H 10T1/2 cells were performed by Han et al. [36]. After 6 Gy at 5 mGy min^{-1} the surviving fraction was 0.7 and the transformation rate was about 5 per 10'000 survivors. Their survival corresponds with the results of our investigations, whereas the transformation rate lies in between the two obtained transformation rates. The value of the transformation without a background of heavily damaged cells is low: 1.05 ± 0.35 transformants per 10'000 survivors, but in the range of the standard error of Han's results.

The C3H 10T1/2 transformation assay is very reproducible compared to other in vitro transformation assays, which was the primary reason for its use in these investigations. C3H 10T1/2 cells are immortalized fibroblasts. This should be considered before comparing our in vitro results with the in vivo situation. Transformation of C3H 10T1/2 cells by high dose-rate X-rays follows a linear-quadratic dose-effect relationship which corresponds to the UNSCEAR report [11], see p. 8.

Radiation-induced carcinogenesis is thought to require multiple genetic alterations subsequent to the initial radiation exposure. DNA double-strand breaks are suggested to be the lesions leading to exchange chromosomal aberrations [108]. The latter are assumed to be predominant cause of oncogenic cell transformation [109]. Classical mutation studies have suggested that specific locus mutations are relatively rare events and for low doses of radiation exposure, the likelihood is small that all relevant changes arise as an immediate consequence of the radiation exposure [110]. Cells exposed to ionizing radiation develop heritable genetic instability. This manifests itself in multiple ways, all of which are typical changes associated with cancer [111]. We investigated genome lability and phenotypic alterations in the C3H 10T1/2 cells subsequent to X-ray exposure with special focus on polyploidization. About 50% of the 8 Gy transformed focal line displayed an abnormal lability in their genomic constitution. We observed polyploidy ranging from hypotriploid to hypododecaploid. The polyploid populations were not usually stable but in

many cases reverted to their parental hypotetraploid state with time in culture. At later passages in transformed C3H 10T1/2 cells isolated after proton-irradiation, Privatera *et al.* found no differences in numerical chromosome distributions between untransformed and transformed cells [112]. Genomic rearrangements of minisatellite DNA have been reported in X-ray transformants of C3H 10T1/2 cells [113]. 40% of the 6 Gy-induced transformants displayed this phenomenon. These authors found no correlation between the appearance of specific genomic rearrangements and tumorigenic potential of the X-ray transformants. We investigated tumor induction by our focal lines in nude mice but found no tumors (unpublished results).

It has been reported that transformation of cells by introduction of oncogenes can increase their radioresistance in association with an increased G2 delay [114]. We examined radiosensitivity of two clones from the focus with the most severe type III phenotype, but no significant difference between either the survival curves of the transformed cells and the parental cells or the duration of their radiation induced cell cycle delays was found (unpublished data, fig. 27).

The transformation rates obtained from the homogeneous β-irradiations correspond to values that have been published in the literature for X-rays. β-rays are expected to act in a similar manner to X-rays. Although, there are some suggestions in the literature of a greater biological efficacy of β-rays. To investigate the unexpectedly high efficacy of Y-90-lymphoma therapy, Macklis *et al.* irradiated various malignant lymphoma lines with 2.5, 5 and 10 Gy of low dose-rate Y-90 β-rays from a homogeneously distributed source in the cell-culture medium [115]. They found in some, but not in all lines, more apoptosis than after high dose-rate γ-radiation. In a Burkitt's lymphoma cell line, tracer doses of P-32 induced massive apoptosis [116] but no dose-response relationships were examined.

Figure 27: Surviving Fractions of Focal and Parental Lines
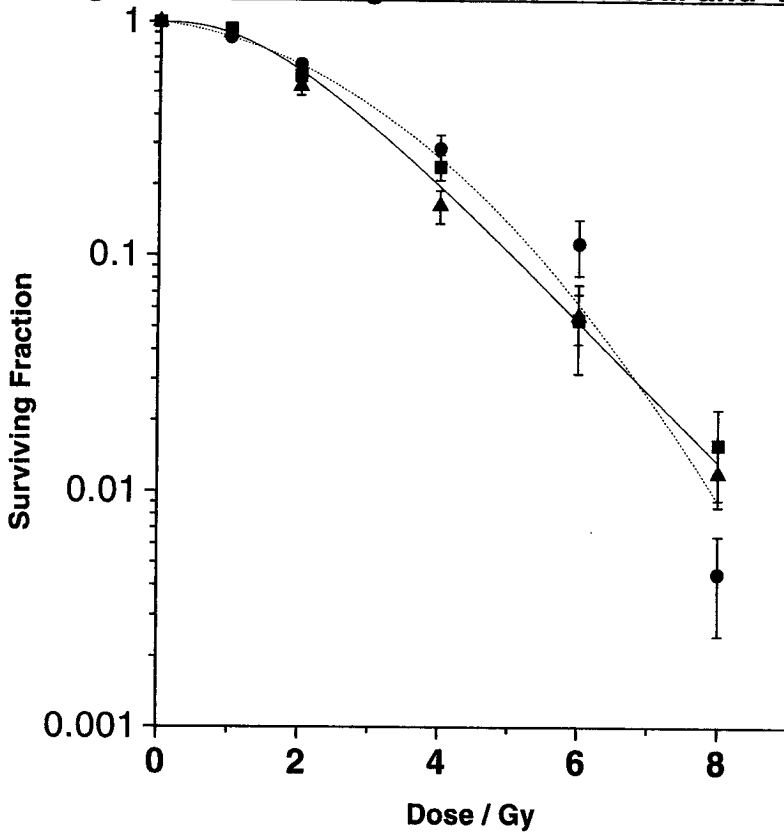
Figure 27: Surviving fraction of two focal lines compared with C3H 10T1/2 cells. Point: C3H 10T1/2 cell; Tiangle: focal line 132-4A; Square: focal line 131-6B. Uncertainties are standard errors of 3 independent experiments. The surviving fractions of the 3 cell lines were not significantly different and all the datas were pooled for the best fit. Solid line is a multitarget fit with $D_0 = 1.4$ Gy and $N = 3.2$, broken line is a linear quadratic fit with $\alpha = 0.08$ Gy^{-1} and $\beta = 0.06$ Gy^{-2}. Both fits are not significantly different.

8. CONCLUSIONS

The enhanced transformation rate of sublethally irradiated C3H 10T1/2 cells with a background of heavily damaged cells implies, that non-stochastic effects in the vicinity of a hot particle can enhance stochastic effects from β-hot-particles. In the lung these effects might be more pronounced than in the skin, since the critical target cells are closer to the particle and the duration of exposure is longer. Although there is some experimental and epidemiological evidence that skin damage by localized beta contamination is enhanced and recovery is prolonged when whole-body γ-irradiation is combined [117].Leszczynski *et al.* [118] exposed very small areas of hairless mouse skin to high dose-rate β- radiadiation and found at the exposed sites overexpression of the tumour supressor gene p53, regularly accompagnied by overexpression of p62$^{c\text{-}fos}$ and p21$^{N\text{-}ras}$. For α- particles the deterministic effects become much more important, since total dose is deposited in a very short range, i.e. most of the dose is „wasted" on dead tissue.

The system developed for the investigation of inhomogeneous irradiation will be useful for future investigations of transformation enhancing factors. With the help of antibodies against certain proteins, exact molecular mechanisms, and with flow cytometric studies, changes in cell cycle can be elucidated. It will be very interesting too, to investigate transformation rate in lower dose ranges, although statistical problems of determining transformation rates close to background transformation rates will make these studies difficult.

9. REFERENCES

1. National Council on Radiation Protection and Measurements, USA. Limits for Exposure to "hot particles", draft 1997

2. National Council on Radiation Protection and Measurements, USA. Limit for Exposure to hot particles on the skin. *NCRP report* **no. 106**. Bethesda, MD, 1990.

3. IAEA, EC and WHO, One decade after Chernobyl: Summing up the consequences of the accident, International Conference, April 1996.

4. Devell, L., Tovedal, H., Bergström, U., Applegren, A., Chyssler, J., and Andersson, L. Initial observations of fallout from the reactor accident at Chernobyl. *Nature*, **321**: 192-193, 1986.

5. Burkart, W. Dose and health implication from particulate radioactivity (hot particles) in the environment. *Bergbau- und Industriemuseum Theuern,* **16**: 121-129, 1988.

6. Hall, E. Radiation Biology for the Radiologist. J.B. Lippincott Comp., Philadelphia, 3th ed., 1988.

7. Herder-Lexikon der Biologie, Spektrum akad. Verlag Heidelberg, Berlin, 1994.

8. Burkart, W. Radiation biology of the lung. *The sci. of the tot. environ,* **89(1/2):** 1-230, 1989.

9. Gehr, P., Im Hof, V., Geiser, M. Reinigungsmechanismen der Luftwege. *Therapeutische Umschau,* **45(5):** 287-295, 1988.

10. Blair, W.J. Overview of ICRP respiratory tract model. *Radiat. Protect. Dosimetry,* **38:** 147-152, 1991.

11. *UNSCEAR Report 1993,* Sources and effects of ionizing radiation. United Nations Scientific Committee on the Effects of Atomic Radiation, Annex F: Influence of dose and dose rate on stochastic effects of radiation, 1993.

12. Risks associated with ionising radiations, in: *Annals of the ICRP,* **22 (1),** 1991.

13. National Council on Radiation Protection and Measurements, USA. Limitation of exposure to ionizing radiation. *NCRP report* **no. 116**. Washington, DC, 1993.

14. Lang, S., Servomaa, K., Kosma, V-M., and Rytömaa, T. Biokinetics of nuclear fuel compounds and biological effects of nonuniform radiation. *Environm. Health Persp.*, **103**: 920-934, 1995.

15. Lang, S., Kosma, V-M., Servomaa, K., Ruuskanen, J. and Rytömaa, T. Tumour induction in mouse epidermal cells irradiated by hot particles. Int. J. Radiat. Biol., **63**: 375-381, 1993.

16. Leszczynski, D., Servomaa, K., Ruuskanen, J., and Rytömaa, T. Radiation-induced frequent concomitant overexpression of p53, p62c-fos and p21n-ras in mouse epidermis. *Cell Prolifer.*, **27**: 517-528, 1994.

17. Reznikoff, C., Brankow, W., and Heidelberger, Ch. Establishement and characterization of a cloned line of C3H mouse embryo cells sensitive to postconfluence inhibition of division. *Cancer Res.*, **33**: 3231-3238, 1973.

18. Reznikoff, C., Bertram, J., Brankow, D., and Heidelberger, C. Quantitative and qualitative studies of chemical transformation of clonal C3H mouse embryo cells sensitive to post confluence inhibition of cell division. *Cancer Res.*, **33**: 3239-3249, 1973.

19. Boreiko, C.J. Initiation and promotion in cultures of C3H 10T1/2 mouse embryo fibroblasts. Mass, M.J. et al. (Eds.) *Carcinogenesis*, **Vol.8**, Raven Press New York, p. 329 - 340, 1985

20. Kennedy, A. R., Mondal, S., and Heidelberger, C. Enhancement of X-ray transformation by 12-O-tetradodecanoyl-phorbol-13-acetate in a cloned line of C3H mouse embryo cells. *Cancer Res.*, **38**: 439-443, 1978.

21. Kennedy, A. R., and Little, J. B. Evidence that a second event in X-ray-induced oncogenic transformation *in vitro* occurs during cellular proliferation. *Rad. Res.*, **99**: 228-246, 1984.

22. Durante, M. Gialanella, G. Grossi, G. F,..., and Tallone, L. Radiation-induced chromosomal aberrations in mouse 10T1/2 cells: dependence on the cell-cycle stage at the time of irradiation. *Int. J. Radiat. Biol.*, **65(4)**: 437-447, 1994.

23. Pazzaglia, S., Saran, A., Pariset, L. Rebessi, S.,.., and Covelli, V. Sensitivity of C3H 10T1/2 cells to radiation-induced killing and neoplastic

transformation as a function of cell cycle. *Int. J. Radiat. Biol.,* **69(1): ** 57-65, 1996.

24. Miller, R. C., Geard, C. R., Geard, M. J., and Hall, E. J. Cell-cycle-dependent radiation-induced oncogenic transformation of C3H 10T1/2 cells. *Rad. Res.,* **130:** 129-133, 1992.

25. Bertram, J. S. Application of retinoid stabilized carcinogen-initiated cells to the quantitation of transformation in the C3H 10T1/2 cell line. *Carcinogen.,* **9:** 327-335, 1985.

26. Bertram, J. S. Role of gap junctional cell/cell communication in the control of proliferation and neoplastic transformation. *Rad. Res.,* **123:** 252-256, 1990

27. Boreiko, J. C., Abernethy, D. J., Rickert, D. E., and Stedman, D. B. Effect of growth state, tumor promoters, and transformation upon intercellular communication between C3H 10T1/2 murine fibroblasts. *Carcinogen.,* **10:** 113-121, 1989.

28. Dunkel, V. C., Schechtman, L. M., Tu, A. S., Sivak, A., Lubet, R. A., and Cameron, T. P. Interlaboratory evaluation of the C3H 10T1/2 cell transformation assay. *Environ. Mol. Mutagen.,* **12:** 21-31 (1988).

29. Hieber, L. Trutschler, K., Smida, J. and Kellerer, A. M. Radiation induced cell transformation: Transformation efficiencies of different types of ionizing radiation and molecular changes in radiation transformants and tumor cell lines. *Environm. Health Persp.,* **88:** 169-174, 1990.

30. Schillaci, M. E., and Carpenter, S. Radiobiology of ultrasoft X-rays. *Rad. Res.,* **118:** 83-92, 1989.

31. Herschmann, H. R., and Brankow, D. W. Ultraviolet irradiation transforms C3H10T1/2 cells to a unique, suppressible phenotype. *Science,* **234:** 1385-1388, 1986.

32. Boreiko, C. J. Methodology for cell transformation assays with C3H 10T1/2 mouse embryo fibroblasts. *J. of Tiss. Cult. Meth.,* **10(3):** 165-172, 1986.

33. Kennedy, A.R. Fox, M., Murphy, G., and Little, J. B. Relationship between X-ray exposure and malignant transformation in C3H 10T1/2 cells. *Proc. Natl. Acad. Sci. USA*, **77**: 7262-7266 (1980).

34. Bettega, D., Calzolari, P., Ottolenghi, A., and Tallone Lombardi, L. Criteria and techniques for analysing cell survival data. *Radiat. Environ. Biophys.*, **30**: 53-70, 1991.

35. Hieber, L. Personal communications

36. Han, A., and Elkind, M. M. Transformation of mouse C3H/10T1/2 cells by single and fractionated dose of X-ray and fission-spectrum neutrons. *Cancer Res.*, **39**: 123-130, 1979.

37. Balcer-Kubicek, E. K., Harrison, G. H., and Thompson, B. W. Repair time for oncogenoc transformation in C3H/10T1/2 cells subjected to protracted X-irradiation. *Int. Journ. Radiat. Biol.*, **51**: 219-226, 1987.

38. Lieser, K. H. Einführung in die Kernchemie, 1. 2nd. ed., Verlag Chemie, Weinheim/Deerfield Beach/Basel, 1980, p. 567 ff.

39. Durham, J. S. VARSKIN MOD2 and SADDE MOD2: Computer codes for assessing skin dose from skin contamination. *NUREG/CR-5873*, **PNL-7913** 1992.

40. Cross, W. G., Ing, H., Freedman, N. O., and Mainville, J. Tables of beta-ray dose distributions in water, air and other media. *Atomic Energy of Canada Limited*, **AECL-7617**, p.40, 1982.

41. Dean, P. N., and Langham, W. H.. Tumorigenicity of small highly radioactive particles. *Health Phys.*, **16**: 79-89; 1969.

42. Tamplin, A. R., and Cochran, T. B. Radiation standards for hot particles, Natural Resources Defense Council, Washington D.C., 1974.

43. Mayneord, W. V., and Clarke, R. H. Quantitative assessment of carcinogenic risks associated with hot particles. *Nature*, **259**: 535-539, 1976.

44. Richmond, C. R. The importance of non-uniform dose-distribution in an organ. *Health Phys.*, **29**: 525-537, 1975.

45. Voelz, G. L., and Lawrence, J. N. P. A 42-y medical follow-up of Manhattan Project plutonium workers. *Health Phys.*, **61 (2):** 181 -190, 1991.

46. International Commission on Radiological Protection. Limits for intakes of radionuclides by workers. Oxford: Pergamon Press; ICRP-Publ. 30, Part1; *Ann. ICRP,* **2 (3/4),** 1979.

47. Falk, R., Suomela, J., and Kerekes, A. A study of hot particles collected in Sweden one year after the Chernobyl accident. *J. Aerosol Sci.,* **19:** 1339-1342, 1988.

48. Charles, M. W., Williams, J. P., and Coggle, J. E. Skin carcinogenesis following uniform and nonuniform beta irradiation. *Health Phys.,* **55:** 399-406 1988.

49. Hopewell, J. W., Sieber, V. K., Heryet, J. C., Wells, J., and Charles, M. W. Dose- and source-size-related changes in the late response of pig skin to irradiation with single doses of beta radiation from sources of differing energy. *Rad. Res.,* **133:** 303-311, 1993.

50. Blizard, E. P., Foderaro, A., Goussev, N. G., and Kovalev, E. E. Extended radiation sources. In Engineering Compendium on Radiation Shielding (R. G. Jaeger, E. P. Blizard, A. B. Chilton, M. Grotenhuis, A. Hönig, Th. A. Jaeger, and H. H. Eisenlohr, Eds.), Vol.I, pp. 363-367. Springer-Verlag, 1968.

51. International Commission on Radiation Units and Measurements. Stopping Powers for Electrons and Positrons, *ICRU Report,* **37:** 160-161; Bethseda, 1984.

52. Elkind, M. M. The initial part of the survival curve. *Rad. Res.,* **71:** 9-23, 1977.

53. Prestwich, W. V., Kennett, T. J., and Kus, F. W. The dose distribution produced by a ^{32}P-coated stent. *Med. Phys.,* **22 (3):** 313-320, 1995.

54. Wells, R. L., and Bedford, J. S. Dose-rate effects in mammalian cells. *Rad. Res.,* **94:** 105-143, 1983.

55. Mitchell, J. B., Bedford, J. S., and Bailey, S. M. Dose-rate effects in mammalian cells in culture. *Rad. Res.,* **79:** 537-551, 1979.

56. Hall, E. J., and Brenner, D. J. The dose-rate effect revisited: radiobiological considerations of importance in radiotherapy. *Int. J. Rad. Oncol. Biol. Phys.,* **21:** 1403-1414, 1991.

57. Wong, J. Y. C., Lawrence, E. W., Demidecki, A. J., Wessels, B. W., and Yan, X. W. Radiobiologic studies comparing yttrium-90 irradiation and external beam irradiation in vitro. *Int. J. Rad. Oncology Biol. Phys.,* **20:** 715-722, 1991.

58. Berger, M.J. Distribution of absorbed dose around point sources of electrons and beta particles in water and other media. Medical Internal Radiation Dose Committee, Pamphlet No. 7, *Journ. Nucl. Med.* **12(5):** 5, 1971.

59. Cross, W.G., Wong, P.Y., and Freedman, N.O. Beta-ray depth dose distributions from incident beams and skin contamination. Health Physics Society Annual Meeting in Anaheim, June, 1990. (see also Varskin Mod 2, Technical Basis).

60. Nagasawa, H., and Little, J. B. Induction of sister chromatid exchanges by extremely low doses of α-particles. *Cancer Res.,* **52:** 6394-6396, 1992.

61. Deshpand, A., Goodwin, E. H., Bailey, S. M., Marrone, B. L., and Lehnert, B. E. Alpha-particle-induced sister chromatid exchanges in normal human lung fibroblasts: Evidence for an extranuclear target. *Rad. Res.,* **145:** 260-267, 1996.

62. Hickman, A. W., Jaramillo, R. J., Lechner, J. F., and Johnson, N. F. α-Particle-induced *p53* protein expression in a rat lung epithelial cell strain. *Cancer Res.,* **54:** 5797-5800, 1994.

63. Servomaa, K., and Rytömaa, T. Malignant transformation of mouse fibroblasts by uranium aerosols released from Chernobyl. In *Frontiers in Radiation Biology* (E. Riklis, Ed.),. pp 589-594. Weinheim, VCH, 1990.

64. Jacobson, M. D. Reactive oxygen species and programmed cell death. *TIBS,* **21:** 83-86, 1996.

65. Han, A., Hill, C. K., and Elkind, M. M. Repair of cell killing and neoplastic transformation at reduced dose rates of ^{60}Co γ-rays. *Canc. Res.*, **40:** 3328-3332, 1980.

66. Terzaghi, M., and Little, J. B. Repair of potentially lethal radiation damage in mammalian cells is associated with enhancement of malignant transformation. *Nature,* **253:** 548-549, 1975.

67. Crompton, N. E. A., Sigg, M. and Jaussi, R. Genome lability in radiation-induced transformants of C3H10T1/2 mouse fibroblasts. *Rad. Res.*, **138:** S105-S108, 1994.

68. Raju, M. R., Eisen, Y., Carpenter, S., and Inkret, W. C. Radiobiology of α particles; III. Cell inactivation by α-particle traversals of the cell nucleus. *Rad. Res.,* **128:** 204-209, 1991.

69. Weichselbaum, R. R., Hallahan, D. E., Sukhatme, V., Dritschilo, A., Sherman M. L., and Kufe, D. W. Biological consequences of gene regulation after ionizing radiation exposure. *J. Natl. Cancer Inst.*, **83:** 480-484, 1991.

70. Coleman, W. B., Throneburg, D. B., Grisham, J. W., and Smith, G. W. Overexpression of c-K-ras, c-N-ras and transforming growth factor beta co-segregate with tumorigenicity in morphologically transformed C3H 10T1/2 cell lines. *Carcinogen.,* **15(5):** 1005-1012, 1994.

71. Sorrentino, V., Drozdoff, V., Zeitz, L., and Fleissner, E. Increased radiation-induced transformation in C3H/10T1/2 cells after transfer of an exogenous c-myc gene. *Proc. Natl. Acad. Sci. USA,* **84:** 4131-4134, 1987.

72. Schwarz, L. C., Damen, J. E., Greenberg, A. H., and Wright, J. A. Altered responsiveness of metastatic versus non-metastatic fibroblasts to heparin-binding growth factors. *Cancer Letters,* **42:** 193-197, 1988.

73. Van Bekkum, D. W., and Bentvelzen, P. The concept of gene transfer-misrepair mechanism of radiation carcinogenesis may challenge the linear extrapolation model of risk estimation for low radiation doses. *Health Physics,* **43:** 231-237, 1982.

74. Hill, C. K., Han, A., and Elkind, M. M. Promoter-enhanced neoplastic transformation after γ-ray exposure at 10 cGy/day. *Rad. Res.*, **199:** 348-355, 1989.

75. Crompton, N. E. A., Barth, B., and Kiefer, J. Inverse dose-rate effect for the induction of 6-thioguanine-resistant mutants in chinese hamster V79-S cells by 60Co gamma rays. *Rad. Res.,* **124**: 300-308, 1990.

76. Kennedy, A. R., Cairns, J., and Little, J. B. Timing of the steps in transformation of C3H 10T1/2 cells by X-irradiation. *Nature,* **307:** 85-87, 1984.

77. Crompton, N. E. A., Hain, J., Jaussi, R., and Burkart, W. Staurosporine and radiation induced G2 cell cycle blocks are equally released by caffeine. *Rad. Res.,* **135:** 372-379, 1993.

78. Smith, G. J., Bell, W. N., and Grisham, J. W. Clonal analysis of the expression of multiple transformation phenotypes and tumorigenicity by morphologically transformed 10T1/2 cells. *Cancer Res.,* **53:** 500-508, 1993.

79. Pollock, E. J., Aaronson, S. A., and Todaro, G. J. X-irradiation of Balb/3T3: Sarcoma-forming ability and virus induction. *Int. J Radiat. Biol.,* **17:** 97-100, 1970.

80. Wheatley, D. N. Pericentriolar virus-like particles in Chinese hamster ovary cells. *J. gen. Virol.,* **24:** 395-399, 1974.

81. Heine, U. I., and Todaro, G. J. New type B retrovirus isolates associated with kinetochores and centrioles of the host cell. *J. Gen. Virol.,* **39:** 41-52, 1978.

82. Heine, U. I., Kramarsky, B., Wendel, E., and Suskind, R.G. Enhanced proliferation of endogenous virus in Chinese hamster cells associated with microtubules and the mitotic apparatus of the host cell. *J. gen. Virol.,* **44:** 45-55, 1979.

83. Benomar, A., Gerlier, D., and DorÁ, J.-F. In vivo activation of mouse macrophages by human melanoma cells. *J. Natl. Cancer Inst.,* **79:** 131-136, 1987.

84. Pöllännen, R., and Toivonen, H. Skin dose calculations for uranium fuel particles below 500 μm in diameter. *Health Phys.,* **68(3):** 401-405, 1995.

85. Terzaghi, M., and Little, J. B. Radiation-induced transformation in a C3H mouse embryo derived cell line. *Cancer Res.,* **36:** 1367-1374, 1976.

86. Klein J. C. Evidence against a direct carcinogenic effect of x-rays in vitro. *J. Natl. Canc. Inst.,* **52:** 1111-1115, 1974.

87. Krump-Konvalinkova V., and Van den Berg, K. J. Leukaemia virus infection promotes fibroblast transformation by normal BALB/c mouse DNA fragments. *Nature,* **287:** 353-   , 1980.

88. Herrlich, P., Ponta, H., and Rahmsdorf, H. J. DNA damage-induced gene expression: signal transduction and relation to growth factor signaling. *Rev. Physiol. Biochem. Pharmacol.,* **119:** 187-223, 1992.

89. UNSCEAR Report 1994, Sources and effects of ionizing radiation. United Nations Scientific Committee on the effects of Atomic Radiation, Appendix B, 1994.

90. Terzaghi-Howe, M. Interactions between cell populations influence expression of the transformed phenotype in irradiated rat tracheal epithelial cellls. *Rad. Res.,* **121:** 242-247, 1990.

91. Randall, K., and Coggle, J. E. Expression of transforming growth factor-β1 in mouse skin during the acute phase of radiation damage. *Int. J. Rad. Biol.,* **68(3):** 301-309, 1995.

92. Kennedy, A. R. Is there a critical target gene for the first step in carcinogenesis? *Environm. Health Persp.,* **93:** 199-203, 1991.

93. Billings, P. C., Shuin, T., Lillehaug J., Miura, T., Roy-Burman, P., and Landolph, J. R. Enhanced expression and state of c-myc oncogene in chemically and X-ray-transformed C3H 10T1/2 Cl8 mouse embryo fibroblasts. *Cancer Res.,* **47:** 3643-3649, 1987.

94. Leuthauser, S. W. C., Thomas, J. E., and Guernsey, D. L. Oncogenes in X-ray-transformed C3H 10T1/2 mouse cells and in X-ray-induced mouse fibrosarcoma (RIF-1) cells. *Int. J. Rad. Biol., 62:* 45-51, 1992.

95. Sherman, M. L., Datta, R., Hallahan, D. E., Weichselbaum, R. R., and Kufe, D. W. Ionizing radiation regulates expression of the c-jun protooncogene. *Proc. Natl. Acad. Sci USA*, **87**: 5663-5666, 1990.

96. Prasad, V. A., Mohan, N., Chandrasekar, B., and Meltz, M. L. Induction of transcription of „immediate early genes" by low-dose ionizing radiation. *Rad. Res.*, **143**: 263-272, 1995.

97. Haimovitz-Friedman, A., Vlodavsky, I., Chaudhuri, A., Witte, L., and Fuks, Z. Autocrine effects of fibroblast growth factor in repair of radiation damage in endothellial cells. *Cancer Res.*, **51**: 2552-2558, 1991.

98. Krämer, M., Sachsenmaier, C., Herrlich, P., and Rahmsdorf, H. J. UV-irradiation-induced interleukin-1 and basic fibroblast growth factor synthesis and release mediate part of the UV Response. *J. Biol. Chem.*, **268(9)**: 6734-6741, 1993.

99. Boesen, J. J. B., Dieteren, N., Bal, E., Lohmann, P. H. M., and Simons, J. W. I. M. A possible factor in genetic instability of cancer cells: stress induced secreted proteins lead to decrease in replication fidelity. *Carcinogen.*, **13(12)**: 2407-2413, 1992.

100. Woloschak, G. E., Chang-Liu, C., and Shearin-Jones, P. Regulation of protein kinase C by ionizing radiation. *Cancer Res.*, **50**: 3963-3967, 1990.

101. Lin, C. S., Goldthwait, D. A., and Samols, D. Induction of transcription from the long terminal repeat of Maloney murine sarcoma provirus by UV-irradiation, X-irradiation and phorbol ester. *Proc. Natl. Acad. Sci. USA,* **87**: 36-40, 1990.

102. Hallahan, D. E., Sukhatme, V. P., Sherman, M. L., Virudachalam, S., Kufe, D., and Weichselbaum, R. R. Protein kinase C mediates X-ray inducibility of nuclear signal transducers EGR1 and JUN. *Proc.Natl.Acad.Sci. USA,* **88**: 2156-2160, 1991.

103. Krauss, R. S., Housey, G. M., Johnson, M. D., and Weinstein, I. B. Disturbances in growth control and gene expression in a C3H 10T1/2 cell line that stably overproduces protein kinase C. *Oncogene,* **4**: 991-998, 1989.

104. Boothman, D. A., Hughes, E. N., and Pardee, A. B. The role of X-ray-induced DNA repair processes in mutagenesis and carcinogenesis. *Mutation and the Environment*, **part E**: 319-327, 1990.

105. Cohen, S. M., and Ellwein, L. B. Cell proliferation in Carcinogenesis. *Science*, **249**: 1007-1011, 1990.

106. Yi, P. N., Evans, H. H., Beer, J. Z., and Rha, C. K. Relationships between mitotic delay and the dose rate of X-radiation. *Rad. Res.*, **140**: 387-392, 1994.

107. Kim, T. A., Cutry, A. F., Kinniburgh, A. J., and Wenner, C. E. Transforming growth factor β1-induced delay of cell cycle progression and its association with growth-related gene expression in mouse fibroblasts. *Cancer Lett.*, **71**: 125-132, 1993.

108. Bryant, P. E., and Johnston, P. J. Restriction-endonuclease-induced DNA double-strand breaks and chromosomal aberrations in mammalian cells. *Mutation Res.*, **299**: 289-296, 1993.

109. Borek, C., Ong, A., Morgan, W. F., and Cleaver, F. E. Morphological transformation of 10T1/2 mouse embryo cells can be initiated by DNA double strand breaks alone. *Mol. Carcinog.*, **4**: 243-247, 1991.

110. Kronenberg, A. Radiation-induced genomic instability. *Int. J. Rad. Biol.*, **66 (5)**: 603-609, 1994.

111. Murnane, J. P. Role of induced genetic instability in the mutagenic effects of chemicals and radiation. *Mutation Res.*, **367**: 11-23, 1996.

112. Privitera, E., Mosna, G., Sala, E., Spiga, I. Gambaro, F., and Ghidoni, A.. Double minute chromosomes and a homogeneously staining chromosome region in C3H 10T1/2 murine cells transformed in vitro by proton radiation. *Cancer Genet. Cytogenet.*, **49**: 75 - 86, 1990.

113. Paquette, P., and Little, J. B. Genomic rearrengements in mouse C3H10T1/2 cells transformed by x-ray, UV-C and 3-methylcholanthren, detected by a fingerprint assay. *Cancer Res.*, **52**: 5788-5793, 1992.

114. Su and Little

115. Macklis, R. M., Beresford, B. A., and Humm, J. L. Radiobiological studies of ^{90}Y-lymphoma therapy. *Cancer*, **73:** 966-973, 1994.

116. Forster, T. H., Allan, D. J., Gobe, G. C., Harmon, B. V., Walsh, T. P., and Kerr, J. J. R. Beta-radiation from tracer doses of ^{32}P induces massive apoptosis in a Burkitt's lymphoma cell line. *Int. J. Rad. Biol.,* **61(3):** 365-367, 1992.

117. Randall, K., and Coggle, J. E. The effect of whole-body γ-irradiation on localized β-irradiation-induced skin reactions in mice. *Int. J. Rad. Biol.,* **62(6):** 729-733, 1992.

118 . Leszczynski, D., Servomaa, K., Lang, S., Kosma, V.-M., and Rytömaa, T. Radiation-induced concomitant overexpression of p53, p62c-fos and p21n-ras in mouse epidermis. *Cell. Prolif.* **27:** 517-528, 1994.

10. APPENDIX

10.1. CURRICULUM VITAE

Name:	Sigg
Prename:	Martina, Noelle
Born:	December 20, 1960 in Schaffhausen
Adress:	Oberdorfstr. 27, 5107 Schinznach-Dorf
	056/ 443 19 49
Place of Birth:	Dörflingen, SH, Switzerland

1967 - 1980:	Primary-, Secundary- and High School in Schaffhausen
	Matura Typ B
1980 - 1986:	Studies in Pharmacy, ETH Zurich
	Diploma as Eidg. dipl. Pharm.
1987 - 1992:	Scientific assistant at the Paul Scherrer Institute (PSI), Institute for Medical Radiobiology of the University of Zurich and the Paul Scherrer Institute, CH - 5232 Villigen PSI
	Doctoral thesis: Stochastic and non-stocastic effects of beta-hot particles in tissue
1988:	Education as „Strahlenschutzsachverständige" at the PSI

Member of the Swiss Society of Radiation Biology and Medical Physics (SGSMP) and of the Swiss Society of Pharmacists (SAV)

Since 1990 co-owner of the „Apotheke Schinznach-Dorf"

10.2. Publications

Reviewed papers

Crompton N.E.A., Sigg M., and Jaussi R.,Genome lability in radiation-induced trans-formants of c3h 10T1/2 mouse fibroblasts, Rad. Research **138:** S105 - S108 (1994).

Sigg M., Crompton N.E.A., and Burkart W., A pure beta line source to assess hot particle effects *in vitro,* Health Phys. **71(2)**: 135-141 (1996).

Sigg M., Crompton N.E.A., and Burkart W., Enhanced transformation in an inhomogeneous radiation field: an effect of the presence of heavily damaged cells, Rad. Research, **148:** 534-547 (1997).

Crompton N.E.A., Emery C.E., Shi Y., Sigg M., and Blattmann H., Radiation-induced genetic instability is not associated with changes in radiosensitivity or cell cycle checkpints in C3H 10T1/2 mouse fibroblasts, Radiat. Environm. Biophysics, *in press.*

Abstracts and Proceedings

Sigg M., Burkart W., Inkorporation von Radioaktivität und Weitergabe an den Säugling, Swiss Med **10,** 1a:52-55 (1988)

Sigg M., Burkart W., Hot Particles: Ein Zellkulturmodell, in: Tagungsbericht Luzern, edited by SGSMP, Luzern: Verlag Max Huber, p. 107 - 111 (1990)

Sigg M., Burkart W., A cell culture model to study radiation effects of hot particles, Experientia **46**: A 16 (1990)

Sigg M., Burkart W., Linear radiation source in cell culture to model hot particles, Radiation Research, a twentieth century perspective I, edited by Chapman J.D. et al. San Diego,CA, 429 (1991)

Sigg M., Burkart W., A cell culture system to study epigenetic effects in an inhomogeneous radiation field , Experientia **47**: A33 (1991)

Sigg M., Burkart W., Evidence for enhanced transformation rate in an inhomogeneous radiation field, Experientia **48**: 404 (1992)

Sigg M., Burkart W., Enhanced transformation rate in an inhomogeneous radiation field, Proc. of the 24th annual meeting of the european society for radiation biology, p. 200 (1992)

Crompton N.E.A., Sigg M., Hain J., Jaussi R., Cell cycle arrest by staurosporine mimics radiation induced G2 delay and predicts the aggresiveness of radiation induced transformation phenotypes, ib., p. 33